



# Bantam Lake

## 2021 Water Quality Monitoring

Prepared for the  
Bantam Lake Protective Association  
Morris, CT  
January 9, 2022

This page has been intentionally left blank.

## EXECUTIVE SUMMARY

Aquatic Ecosystem Research (AER) was engaged by the Bantam Lake Protective Association (BLPA) to conduct monthly water quality monitoring and biweekly cyanobacteria monitoring from April through October of 2021 at two sites on Bantam Lake (North Bay or NB, and Center Lake or CL). Two additional sites were also visited during each sampling event where in-situ data (Secchi transparency, temperature, oxygen, etc.) were collected (Point Folly or PF, and South Bay or SB). Supplemental data were also collected at the same sites by James Fischer from the White Memorial Environmental Center; those data were incorporated into this analysis.

- Between late April and late May, the water column became stratified at all sites.
  - For the remainder of the season, the SB site water column was intermittently stratified (i.e., it was mixed more often than it was stratified during the season).
    - Oxygen concentrations at the SB site were >2mg/L at all depths with the exception of bottom strata (4.5m of depth) on April 27<sup>th</sup>.
  - The CL and PF sites remained stratified for all visits through late August, but were mixed for the balance of the season by mid-September.
    - Oxygen concentrations of <1mg/L were measured from the 6m strata to the bottom (8m) at the CL site from June 23<sup>rd</sup> through late August.
    - At the PF site, similar oxygen concentrations were observed with the one difference being that a <1mg/L measurement at bottom (6.5m) occurred in mid-September.
  - The NB site was similarly stratified with the exception of August 10<sup>th</sup> when it was mixed; it was stratified again six days later.
    - At the 6m strata of the NB water column, oxygen levels of <1mg/L were measured from late June to late August; but the 5m stratum was only found at that level on July 19<sup>th</sup>, August 16<sup>th</sup>, and August 31<sup>st</sup>.
  - The 2021 season was marked by periods of warming followed by cooling/mixing in epilimnetic strata from June 8<sup>th</sup> through August 16<sup>th</sup>.
- Epilimnetic trophic variables generally reflected a late-mesotrophic to eutrophic system.
  - Average Secchi disk transparencies were >2.4m from late April through early August, and ≤1.9m from mid-August to late October.
    - The lake average for the two periods of time were 2.98m and 1.77m, respectively; the first is characteristic of late-mesotrophic conditions and the latter is characteristic of eutrophic conditions.
  - Average epilimnetic total phosphorus concentrations were 22.1 and 25.0µg/L at the NB and CL sites, respectively and characteristic of late mesotrophic conditions.



- Average hypolimnetic concentrations were 46 and 110µg/L at the NB and CL sites, respectively, and capable of supporting eutrophic to highly-eutrophic algal productivity.
    - The highest concentrations were measured on July 19<sup>th</sup> and August 16<sup>th</sup>.
  - Season average epilimnetic total nitrogen was 457 and 460µg/L at the NB and CL sites, respectively, and characteristic of mesotrophic conditions.
    - Redfield ratios indicated the lake was, on average, phosphorus limited.
  - Average hypolimnetic total nitrogen concentrations were 501 and 675mg/L at the NB and CL sites.
    - Concentrations increased with time and reached their maximum levels on August 13<sup>th</sup>.
    - The highest hypolimnetic ammonia concentrations were measured on July 19<sup>th</sup> and August 16<sup>th</sup>.
- Cyanobacteria cell concentrations and relative phycocyanin concentrations increased steadily from the start of the season through July 19<sup>th</sup>.
  - Following the first copper sulfate treatment on July 29<sup>th</sup>, cell concentrations and phycocyanin levels decreased but subsequently surpassed pretreatment levels after two weeks.
  - Cyanobacteria cell concentrations, on average, exceeded 100,000 cells/mL several times between mid-August and mid-September.
  - Microcystin concentrations measured biweekly from June 8<sup>th</sup> to October 28<sup>th</sup> at the NB and CL sites, were all below the State-recommended maximum limit for reopening beaches closed due to a harmful algal bloom.
  - *Aphanizomenon* spp. was the dominant cyanobacteria for much of the season.
    - *Dolichospermum* spp. became more important later in the season.
    - *Microcystis* spp., *Woronichinia* spp., and several others were commonly observed in samples.
    - These genera are thought to be toxigenic, most of them regulate buoyancy and can utilize elemental nitrogen.
- Specific conductance was variable throughout the season
  - The April 27<sup>th</sup> average of 203µS/cm increased to 209µS/cm by June 23<sup>rd</sup>, decreased between July 19<sup>th</sup> and August 3<sup>rd</sup>, and then increased to 195µS/cm by August 31<sup>st</sup>.
  - By September 13<sup>th</sup>, the surface strata average had decreased to 170µS/cm, and was 164µS/cm by October 28<sup>th</sup>.
  - Hypolimnetic levels began to increase above epilimnetic levels in June at the CL and PF sites.

- Highest hypolimnetic levels were measured between mid-July and Late August.
- Oxidation-reduction potentials below the thermocline were regularly <200mV, especially in July and August at the NB, CL, and PF sites.
  - At <200mV, iron is reduced and the phosphorus that is chemically bound to the iron in lake sediments becomes soluble and takes the form (phosphate) that algae and cyanobacteria can utilize.
  - Ferrous iron concentrations in the hypolimnion were high in July and twice as high in August at the CL site, and high in August at the NB site.
- Certain base cations and anions were more variable during the season while others were less variable.
  - Sodium and chloride levels were more variable, they decreased over time, and were lowest in September and October.
  - Calcium and magnesium concentrations were more conservative.
  - Epilimnetic and hypolimnetic alkalinity levels increased from April 27<sup>th</sup> through August 16<sup>th</sup>, but were lower in September and October.
    - Hypolimnetic alkalinity levels were notably higher than epilimnetic levels from June 23<sup>rd</sup> through August 16<sup>th</sup> and likely due to biologically mediated reduction reactions associated with anaerobic respiration in lake sediments.
- A number of noteworthy findings were discussed and included:
  - Phosphorus mass balance calculations revealed that the September 13<sup>th</sup> mass for the entire water column was very low and comparable to early season (April and/or May) masses in 2018 and 2019.
    - The two major storm events in late August and early September may have temporarily purged nutrients from the lake.
    - Phosphorus levels rebounded by October 12<sup>th</sup>.
  - The August 16<sup>th</sup> total water column mass, which was largely residing in the hypolimnion, was the greatest mass calculated for any month over the last 4 years.
  - Compensation depths were plotted over time with corresponding locations of the thermocline.
    - Compensation Depths were below the thermocline from late April through early July at the CL and PF sites, and through mid-July at the NB site.
      - Afterwards, Compensation Depths were above the thermocline when the lake was still stratified.
      - This timing lines up with the increases in cyanobacteria cell concentrations and high relative phycocyanin concentrations starting in July.

- Growth of cyanobacteria genera that can regulate buoyancy is stimulated when the Compensation Depth is within the mixed epilimnetic layer.
- Maximum RTRM values were plotted over time for both 2020 and 2021.
  - The 2020 season occurred during draught conditions and had only one significant storm event, while 4 major storm events occurred in 2021.
  - The seasonal pattern of stratification and mixing is appreciably impacted by the types of storm events experienced in 2021 at Bantam Lake.
- Lastly, relative cyanobacteria growth rates and relative phycocyanin concentrations were plotted over time.
  - Decreases in growth rates and relative phycocyanin levels were detected following the copper sulfate treatments of July 29<sup>th</sup> and August 24<sup>th</sup>.
  - Both indicators increased after approximately two weeks.
- Recommendations going forward are provided at the end of this report.
  - Some included modifications to this monitoring program.
  - Support for developing a QAPP for lake and watershed monitoring outlined in the States' TMDL study is expressed.

## TABLE OF CONTENTS

Executive Summary.....	2
Introduction .....	11
Historical Water Quality Studies.....	11
CT DEEP's TMDL Study and Watershed-Based Plan.....	12
Current Water Quality Concerns.....	12
Bantam and Climate.....	13
Methods.....	13
Monthly Water Quality Monitoring.....	13
Cyanobacteria Monitoring.....	14
Additional Data Collections.....	15
Mixing and Stratification.....	16
Temperature and Oxygen Profiles .....	17
Trophic Data.....	21
Chlorophyll-a .....	21
Secchi Transparency and Compensation Depth.....	22
Total Phosphorus.....	24
Total Nitrogen.....	25
Redfield Ratios .....	27
Algae and Cyanobacteria Dynamics.....	27
Cyanobacteria Cell Concentrations and Relative Biomass.....	29
Algal Taxa and Genera.....	30
Cyanobacteria Spatial and Temporal Distribution.....	34
Cyanotoxin Monitoring.....	36
Bantam Lake Chemistry .....	36
Specific Conductance.....	37
Oxidation-Reduction Potential .....	40
Base Cations and Chloride .....	41
Alkalinity and pH.....	42
Iron and Manganese .....	45
Major Findings.....	47
Phosphorus Mass Dynamics.....	47
Compensation Depth and Cyanobacteria .....	49
	7



Water Column Stability and Cyanobacteria .....	50
Cyanobacteria Productivity .....	51
Other Considerations of Cyanobacteria Genera.....	53
Other Water Quality Characteristics .....	55
Recommendations .....	57
References.....	58

## LIST OF FIGURES

Figure 1. Reconstruction of Bantam Lake trophic status between ca 1857 and 1991 .....	12
Figure 2. Locations of the sampling sites on Bantam Lake during the 2020 season ...	16
Figure 3. Isopleth plots of temperature at the NB (Site 1), CL (Site 2), PF (Site 3) and SB (Site 4) sites on Bantam Lake for the 2021 season .....	19
Figure 4. Isopleth plots of dissolved oxygen at the NB (Site 1), CL (Site 2), PF (Site 3) and SB (Site 4) sites on Bantam Lake for the 2021 season.....	20
Figure 5. Chlorophyll-a concentrations measured at the North Bay (NB) and Center Lake (CL) sites on Bantam Lake in 2021.....	22
Figure 6. Secchi disk transparency measurements at the North Bay (NB), Center Lake (CL), Point Folly (PF), and South Bay (SB) sites in 2021.....	23
Figure 7. Total phosphorus concentrations in the epilimnion (Epi), metalimnion (Meta), and hypolimnion (Hypo) at the North Bay Site (top), and Center Lake Site (bottom) of Bantam Lake in 2021.....	24
Figure 8. Total nitrogen concentrations in the epilimnion (Epi; left column), metalimnion (Meta; middle column), and hypolimnion (Hypo; right column) of the North Bay (NB; top row) and Center Lake (CL; bottom row) sites of Bantam Lake in 2021.....	26
Figure 9. Cyanobacteria cell concentrations at the North Bay (NB) and Center Lake (CL) sites in 2021.....	28
Figure 10. Relative phycocyanin concentrations at the North Bay (NB), Center Lake (CL), Point Folly (PF), and South Bay (SB) sites in 2021.....	28
Figure 11. Algal specimens collected from Bantam Lake in 2021.....	32
Figure 12. Specimens of cyanobacteria genera collected from Bantam Lake in 2021 ....	33
Figure 13. Isopleth plots of relative phycocyanin concentration at the NB (Site 1), CL (Site 2), PF (Site 3) and SB (Site 4) sites on Bantam Lake for the 2021 season .....	35
Figure 14. Isopleth plots of specific conductance at the NB (Site 1), CL (Site 2), PF (Site 3) and SB (Site 4) sites on Bantam Lake for the 2021 sea-son .....	38



Figure 15. Isopleth plots of oxidation-reduction potential at the NB (Site 1), CL (Site 2), PF (Site 3) and SB (Site 4) sites on Bantam Lake for the 2021 season.....	39
Figure 16. Concentrations of base cations and anions (left) and averages for the season (right) for the NB site (top) and CL site (bottom).....	42
Figure 17. Alkalinity concentrations in the epilimnion (Epi), metalimnion (Meta), and hypolimnion (Hypo) at the North Bay Site (top), and Center Lake Site (bottom) of Bantam Lake in 2021.....	43
Figure 18. Epilimnetic (Epi), metalimnetic (Meta), and hypolimnetic (Hypo) pH at the North Bay (NB) site and CL site.....	44
Figure 19. Epilimnetic (Epi) and hypolimnetic (Hypo) iron concentrations at the North Bay (NB; top) and Center Lake (CL; bottom) sites of Bantam Lake in 2021.....	45
Figure 20. Epilimnetic (Epi) and hypolimnetic (Hypo) manganese concentrations at the North Bay (NB; top) and Center Lake (CL; bottom) sites of Bantam Lake in 2021.....	46
Figure 21. Mass of total phosphorus by strata (epilimnion = Epi, metalimnion = Meta), and hypolimnion = Hypo) on each sampling event from 2018 to 2021.....	47
Figure 22. Area of the water column at the NB (top), CL (middle) and PF (bottom) sites above the Compensation Depth (shaded in green).....	49
Figure 23. Maximum RTRM scores plotted over time in the water column of the North Bay (NB), Center Lake (CL), Folly Point (FP), and South Bay (SB) sites during the 2020 (top) and 2021 (bottom) seasons.....	51
Figure 24. Relative cyanobacteria growth rates (Rel Cyan Growth; red line) and relative phycocyanin concentrations (Rel Phycocyanin; cyan bars) at the four sites on Bantam Lake during the 2021 sampling season.....	52
Figure 25. Ferrous iron concentrations in the hypolimnion of the North Bay and Center Lake sites in the 2018, 2019, 2020, and 2021 seasons.....	56

## LIST OF TABLES

Table 1. Summary of data collections for Bantam Lake in 2020 used in this report .....	15
Table 2. Trophic classification criteria used by the Connecticut Experimental Agricultural Station (Frink and Norvell, 1984) and the CT DEP (1991) to assess the trophic status of Connecticut lakes.....	21
Table 3. Algal genera identified in from the plankton net samples and whole water samples collected at the NB and CL sites on Bantam Lake in 2021.....	31
Table 4. Microcystin concentrations in µg/L in samples collected at Bantam Lake in 2021.....	36
Table 5. Average water quality characteristics in the epilimnion of Bantam Lake from the early 1990s, 2018, 2019, 2020, and 2021 .....	56



This page has been intentionally left blank.

## INTRODUCTION

Bantam Lake is a 966-acre waterbody located in Towns of Litchfield and Morris, Connecticut; and, is the largest natural lake in the State. Geologically, it is situated in the Western Uplands of Connecticut (Bell 1985, Canavan & Siver 1995). That geological region has an erosion resistant, crystalline bedrock comprised of schists, gneiss, granite gneiss, and granofels (Healy & Kulp 1995).

The watershed of Bantam Lake is 20,218 acres resulting in a watershed to lake ratio of approximately 21. In a 1995 survey, land use was characterized as mainly deciduous forest and agriculture lands with smaller areas of medium-density residential land use, wetlands, and coniferous forests (Healy & Kulp 1995). Much of the shoreline is lined with homes, beaches, and several camps. There is also open space along the northern shoreline, which is owned by the White Memorial Foundation.

### *Historical Water Quality Studies*

Earliest known assessments of Bantam Lake occurred in the late 1930s (Deevey 1940). That study and several others occurring over the next 70 years (Frink & Norvell 1984, Canavan & Siver 1994, 1995, Healy and Kulp 1995) included Bantam Lake as part of statewide surveys of Connecticut Lakes that used standard in-situ measurements and laboratory analyses of water samples to develop records of water quality. These studies resulted in important historical water quality baselines for many of Connecticut's lakes. Several of those statewide surveys have been compiled in Canavan and Siver (1994, 1995).

A paleolimnological study of Bantam Lake's water quality used statistical inference models and the remains of fossil bearing algae – layered chronologically in a sediment core – to estimate changes in water quality over time (e.g., trophic level, conductivity levels, and pH, over time; Siver 1993, Siver and Marsicano 1996). The oldest sediments in the Bantam sediment core dated back to *ca* 1857 (Fig. 1).

Based on the earliest fossil assemblages, Bantam Lake was oligotrophic to early mesotrophic from *ca* 1857 through *ca* 1898 (Fig. 1). Subsequently, the lake's trophic status changed; by *ca* 1926 Bantam Lake was mesotrophic. The lake became more eutrophic between *ca* 1946 and *ca* 1964. The fossil assemblages near the top of the core dated to *ca* 1991 and indicated eutrophic conditions.

Bantam Lake has continued to exhibit eutrophic characteristics resulting in the high levels of algal productivity that have become one of the primary management concerns of the Bantam Lake Protective Association (BLPA). High concentrations of cyanobacteria and bloom-like conditions are common between the midsummer and fall periods of the recreational season. This has resulted in the State of Connecticut including Bantam Lake in the State's list of impaired waterbodies, and cites algae, chlorophyll, and nutrients as the causes of impairments (CT DEEP 2020).

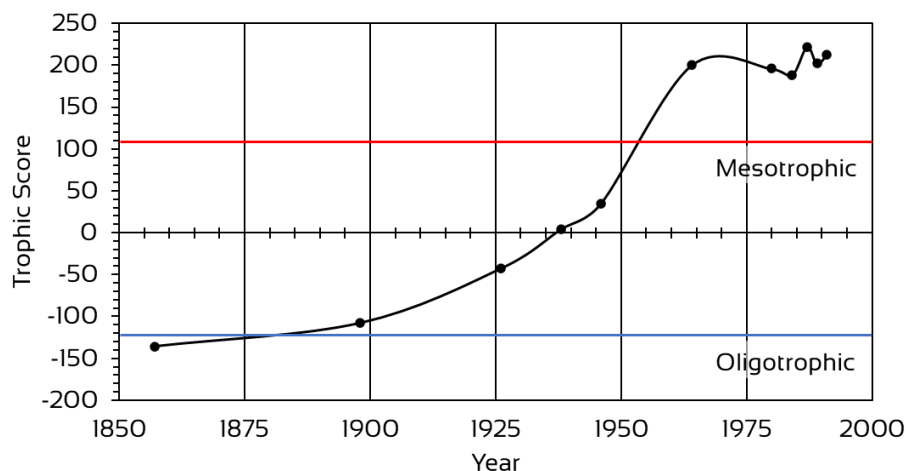


Figure 1. Reconstruction of Bantam Lake trophic status between ca 1857 and ca 1991. The blue horizontal line represents the division between oligotrophic and mesotrophic lakes; and the red horizontal line represents the division between mesotrophic and eutrophic lakes based on a trophic score (Siver and Marsicano 1996).

#### *CT DEEP's TMDL Study and Watershed-Based Plan*

Recent efforts at Bantam Lake by the Connecticut Department of Energy of Environmental Protection, in conjunction with the US EPA, and the BLPA included a *Total Maximum Daily Loading (TMDL) Study* and a *Watershed-Based Plan* (CT DEEP 2021). The TMDL study and watershed plan provide a wealth of information on: 1) the lake and watershed; 2) sources of the nutrients that impair the lake; and 3) measures to reduce nutrient export to the lake. Recommendations are also provided on future lake and watershed monitoring efforts.

#### *Current Water Quality Concerns*

Harmful algal blooms or HABs, have become a key issue in lake management over the last 20 year because of the risk they present to ecosystem and public health. In addition to depletion of oxygen from the water column following a bloom, many genera of cyanobacteria are toxigenic. The cyanotoxins are generally grouped into one of several categories: hepatotoxin that cause liver damage, neurotoxins that have been associated with neurological disorders like Amyotrophic Lateral Sclerosis (ALS), and others in groups classified as dermatoxins, cytotoxins, and endotoxins. The State of Connecticut provides a useful summary on cyanobacteria, the toxins they produce, and standards by which municipal health department can assess conditions at public beaches (CT DPH & CT DEEP 2019). If efforts to manage cyanobacteria growth and minimize risk, two copper sulfate treatments were undertaken during the 2021 season. The first occurred on July 9<sup>th</sup>, and second on August 24<sup>th</sup>.

## *Bantam and Climate*

The impacts of changing climate on lake ecosystems has also become an important topic in lake research and management (e.g., Kortmann and Cummins 2018, Siver et.al. 2018, Kortmann 2020). Some of those impacts include the increase in frequency and intensity of harmful cyanobacteria algae blooms (Ho et.al. 2019, Burford et.al. 2020).

Climate change has been characterized by increases in the intensity and frequency of climate-related events, e.g., longer and more severe periods of draught and more frequent and intense storms. Much of the 2020 season occurred during moderate to extreme draught conditions in Connecticut (NIDIS 2021). The 2021 season experienced more frequent named storms including Tropical Storm Elsa on July 8<sup>th</sup>, Tropical Storm Fred on August 19<sup>th</sup>, Tropical Storm Henri on August 22<sup>nd</sup>, and Hurricane Ida on September 1<sup>st</sup>. Understanding the climate-related impacts is becoming increasingly more important with time.

Since 2018, Aquatic Ecosystem Research (AER) has been engaged by the BLPA to conduct seasonal water quality and cyanobacteria monitoring, and report on it. Below, we report on the results of the 2021 monitoring programs. This report includes a discussion of the methods, describes, assesses, and interprets results of our data collections, provides a discussion of major findings, and provides recommendations for future management directions and initiatives.

## METHODS

### *Monthly Water Quality Monitoring*

Four sampling sites (Fig. 2) were visited six times each between April and October of 2021. Dates of data and water sample collections were: April 27<sup>th</sup>, May 25<sup>th</sup>, June 23<sup>rd</sup>, July 19<sup>th</sup>, August 16<sup>th</sup>, September 13<sup>th</sup> and October 12<sup>th</sup>. Sites were identified as North Bay (NB), Center Lake (CL), Point Folly (PF), and South Bay (SB). Maximum depths were approximately 6 meters (m), 8m, 6.5m, and 4.5m at the NB, CL, FP, and SB sites, respectively.

During each site visit, Secchi transparency was measured with a 26cm diameter Secchi disk. Additionally, vertical profile data for six water column properties were collected using a Eureka Manta II Multiprobe. Profiled data were measured at 0.5m from the surface and at one-meter intervals down to 0.5m above the bottom; profile data included the following variables: temperature (°C), dissolved oxygen (mg/L), percent oxygen saturation (% O<sub>2</sub>), specific conductance (µS/cm), pH, oxidation-reduction potential, and relative cyanobacteria concentration.

Water samples were collected at NB and CL sites during visits and analyzed for the variables listed in Table 1 by a State-certified laboratory with the exception of algae



samples, which were analyzed by AER (see below). Water samples were collected using two different methods and at several depths in the water column. For nutrient and alkalinity analyses, samples were collected with a horizontal Van Dorn water sampler at 1m below the surface (epilimnion), at approximately 0.5m above the sediment-water interface (hypolimnion), and at the thermocline, which was determined using the vertical temperature profiles collected at each site on each sample date. For iron (Fe) and manganese (Mn), samples were collected with the Van Dorn sampler at 1m below the surface and 0.5m above the sediment water interface. For the base cations of sodium ( $\text{Na}^+$ ), potassium ( $\text{K}^+$ ), calcium ( $\text{Ca}^{2+}$ ), magnesium ( $\text{Mg}^{2+}$ ), and the anion chloride ( $\text{Cl}^-$ ), samples were collected from 1m below the surface. All samples were kept on ice in a cooler until delivered to a State-certified lab for analyses.

For chlorophyll-*a*, a weighted tube sampler was used to collect and integrate water from the top three meters of the water column at the NB and CL sites. All samples were kept on ice in a cooler until delivered to a State-certified lab for analyses.

### *Cyanobacteria Monitoring*

Pelagic algae samples were collected on 14 different dates in 2021, including the dates water quality data and samples were collected (Table 1). Samples for algae analyses were collected at the NB and CL sites by integrating the top three meters of the water column with a 3-meter-long sampling tube. Samples were treated with Lugol's solution and kept on ice. Samples were later treated with hydrostatic pressure back in the AER laboratory to collapse gas vesicles that might make cells positively buoyant (Lawton et al. 1999).

When necessary, measured volumes of the preserved whole water samples were concentrated into smaller measured volumes with centrifugation and a vacuum pump / filtration flask system. This step was omitted when cyanobacteria concentrations appeared high based on a visual assessment at the lake or on low Secchi disk transparency. A known portion of those concentrates or whole water samples were pipetted into a counting chamber and genus-level algal cell enumerations were performed by counting algae cells in a subset of fields within the counting chamber slide using an inverted Nikon Diaphot research microscope. Those counts were then corrected to be reflective of the whole sample.

Additionally, a 10 $\mu\text{m}$  plankton net was used to collect a concentrated algal sample from within the top 3m of the CL water column. Those samples were examined and important genera photographed in the laboratory using a Wolfe Digivi™ CVM Microscope with Motic Images Plus 3.0 software.

During each algae sample collection visit, Secchi transparency and vertical profile data were collected at NB, CL, FP, and SB sites. A total of 14 samples for algal analyses were collected at the NB and CL sites in 2021.

Table 1. Summary of data collections for Bantam Lake in 2020 used in this report. NB = North Bay Site, CL = Center Lake Site, FP = Folly Point Site, and SB = South Bay Site. Chl-*a* = chlorophyll-*a*.

2020 Dates	Profiles and Secchi	Algae	Nutrients & Alkalinity	Iron & Manganese	Chl- <i>a</i> , Cations, Chloride
27-Apr-21	NB, CL, FP, SB	NB, CL	NB, CL	NB, CL	NB, CL
12-May-21	NB, CL, FP, SB	NB, CL			
25-May-21	NB, CL, FP, SB	NB, CL	NB, CL	NB, CL	NB, CL
8-Jun-21	NB, CL, FP, SB	NB, CL			
23-Jun-21	NB, CL, FP, SB	NB, CL	NB, CL	NB, CL	NB, CL
28-Jun-21*	NB, CL, FP, SB				
6-Jul-21	NB, CL, FP, SB	NB, CL			
16-Jul-21*	NB, CL, FP, SB				
19-Jul-21	NB, CL, FP, SB	NB, CL	NB, CL	NB, CL	NB, CL
3-Aug-21	NB, CL, FP, SB	NB, CL			
10-Aug-21*	NB, CL, FP, SB				
16-Aug-21	NB, CL, FP, SB	NB, CL	NB, CL	NB, CL	NB, CL
31-Aug-21	NB, CL, FP, SB	NB, CL			
13-Sep-21	NB, CL, FP, SB	NB, CL	NB, CL	NB, CL	NB, CL
29-Sep-21	NB, CL, FP, SB	NB, CL			
12-Oct-21	NB, CL, FP, SB	NB, CL	NB, CL	NB, CL	NB, CL
28-Oct-21	NB, CL, FP, SB	NB, CL			

\* Data collections by James Fischer of the White Memorial Conservation Center. All others by AER.

### *Additional Data Collections*

Addition Secchi transparency and profile data were collected by James Fischer, Director of Research for the White Memorial Conservation Center. The White Memorial Conservation Center is a partner and advisor to the Bantam Lake Protective Association. The data collected by Mr. Fischer facilitated greater temporal resolution in assessments of seasonal Secchi transparencies, and temperature/oxygen dynamics in the water column. Those data have been incorporated into the results and discussions below. Specific dates of AER's and Mr. Fischer's site visits and data collections are indicated in Table 1.



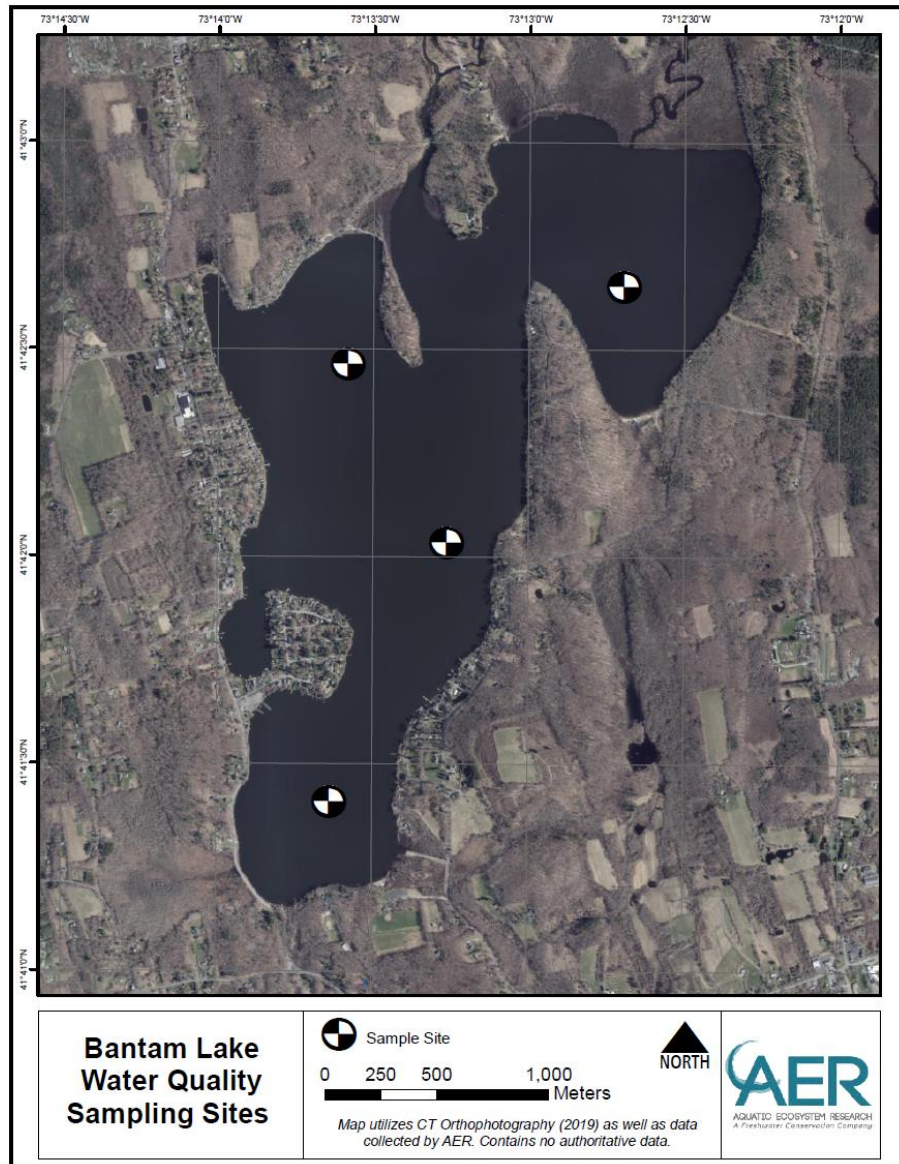


Figure 2. Locations of the sampling sites on Bantam Lake during the 2020 season. NB = North Bay Site, FP = Folly Point Site, CL = Center Lake Site, and SB = South Bay Site.

### *Mixing and Stratification*

Patterns of water column mixing and resistance to mixing (or stratification) were assessed using temperature profile data. Resistance to mixing, which is an assessment of the ability of two different water volumes – that differ in temperature and density – to mix, was calculated using the Relative Thermal Resistance to Mixing (RTRM) formula:  $(D_1 - D_2)/(D' - D^0)$ , where  $D_1$  is the density of upper water volume,  $D_2$  is the density of the lower water volume,  $D'$  is the density of water at 5°C, and  $D^0$  is the density of water at 4°C.



## TEMPERATURE AND OXYGEN PROFILES

Water quality variables measured throughout the water column are being provided digitally to the BLPA. We have displayed many of those data below as isopleths where a variable (e.g., temperature) is displayed as shades of colors throughout the water column at each depth and for all dates when data were collected. Values were then interpolated between depths and dates. Variables of the same value (and color) were connected between dates irrespective of depth to create a theoretical representation of changes throughout the water column over time.

Water temperature data provides a view into the thermal characteristics of the lake and the patterns of stratification resulting from temperature/density differences between depths or strata. In shallow New England lakes or shallow sites in a deep lake, stratification can occur but may be short in duration because wind energy has the potential to mix the water column. In deeper lakes or sites, stratification is not as easily deteriorated by wind energy.

When a lake is stratified, a middle transitional layer (aka metalimnion) separates the upper warmer layer (aka epilimnion) from lower colder waters below (aka hypolimnion). Within the boundaries of the metalimnion resides the thermocline, which is the stratum where the temperature/density change and resistance to mixing are the greatest with increasing depth. Stratified conditions can usually persist in deeper lakes or sites for the entire summer and into the fall until turnover mixes the water column.

An oxygen concentration of 5mg/L is generally considered the threshold that defines favorable conditions for most aerobic organisms in freshwater systems. As concentrations decrease below that threshold, conditions become stressful for many forms of life. Minimum oxygen requirements for fisheries in Connecticut's lakes and ponds range from 4 to 5mg/L for cold-water fish (e.g., trout), 2mg/L for cool-water fish (e.g., walleye), and 1 to 2mg/L for warm-water fish (e.g., bass and panfish; Jacobs and O'Donnell 2002).

The loss or absence of oxygen at the bottom of the water column modifies the chemical environment as compared to conditions when oxygen is present. These modifications result in the dissolution of compounds (e.g., iron phosphate) from the sediments to the interstitial waters and – then, by diffusion – to the waters above the sediments.

The water column at all four sites was isothermal and coldest from April 27<sup>th</sup> through May 12<sup>th</sup> (Fig. 3). Temperatures on the former date were between 10 and 11°C, and between 13 and 14°C on the later date. It was during this period when the highest oxygen concentrations were recorded throughout the water column (Fig. 4). At the NB, CL, and PF sites, concentrations were between 9 and 11mg/L. At the SB site on April 27<sup>th</sup>, concentrations between 11 and 11.3mg/L were measured throughout the water column excluding the very bottom (i.e., 4.5m of depth) where the concentration was <1mg/L.

By May 25<sup>th</sup>, temperatures in specific strata of the water column began to become discrete. Surface waters down to 3 or 4m of depth had warmed to between 19 and 20°C.

A thermocline developed at all sites by this date and temperatures below it were between 13 and 14°C depending on maximum depth of each site. An upper metalimnetic boundary was detected at the PF site. The start of stratification between May 12<sup>th</sup> and May 25<sup>th</sup> coincided with a reduction of oxygen levels below the lower metalimnetic boundary or thermocline. The lowest concentration of 1.9mg/L was measured at the lowest strata of the PF site.

A warming of the upper strata of the water column by June 8<sup>th</sup> was concurrent with a shift in the thermocline and upper metalimnetic boundary – if different from the thermocline – to a higher position in the water column at the NB, CL, and PF sites. At the SB site, the thermocline did not shift relative to its position on May 25<sup>th</sup>, but an upper metalimnetic boundary was detected between 2 and 3m of depth. Oxygen concentrations on June 8<sup>th</sup> were similar to those observed on May 25<sup>th</sup>.

From June 8<sup>th</sup> to June 23<sup>rd</sup> – and through July 6<sup>th</sup> – epilimnetic water temperatures cooled by 1 to 2°C. Mixing and a downward shift of the thermocline and metalimnetic boundaries at the NB, CL, and PF sites occurred, which also resulted in a breakdown of stratification in the SB site water column. It was during this period when oxygen concentrations decreased to levels of <1mg/L near the bottom at all but the SB site. Anoxic conditions were measured from the 6m strata to the bottom at the three sites on July 6<sup>th</sup>. Hypolimnetic oxygen levels at the SB site were often lower than corresponding epilimnetic levels but were never <2mg/L over the course of the season except on April 27<sup>th</sup>.

From July 6<sup>th</sup> through July 19<sup>th</sup>, surface water temperatures warmed by approximately 2 to 2.5°C (Fig. 3). The rapid warming resulted in the formation of a second thermocline between 2 and 3m of depth on July 16<sup>th</sup> at the CL and PF sites. On July 19<sup>th</sup>, the second thermocline was not observed but that stratum was at the approximate position of the upper metalimnetic boundary and/or thermocline. During this time, hypolimnetic strata starting at 5m of depth at the NB site, and starting at 6m of depth at the CL and PF sites, exhibited oxygen concentrations of <1mg/L.

Another period of cooling and mixing followed by warming of the surface strata occurred following July 19<sup>th</sup>. Epilimnetic temperatures on August 3<sup>rd</sup> were 1.6°C to 2.25°C lower than those on July 19<sup>th</sup>. Temperatures in the same strata on August 10<sup>th</sup> and August 16<sup>th</sup> had increased and exceeded 24°C and 25°C, respectively at all sites. Stratification at the NB water column was not detected on August 10<sup>th</sup> but was detected on August 16<sup>th</sup>. At the CL site, the upper metalimnetic boundary moved up in the water column; at the PF site, the upper metalimnetic boundary and thermocline both shifted upward. The SB water column was mixed for the remainder of the season after July 19<sup>th</sup>. Hypolimnetic strata continued to be anoxic at the NB, CL and PF sites. At the CL site, anoxic conditions were observed above the thermocline after August 3<sup>rd</sup> (Fig. 4).

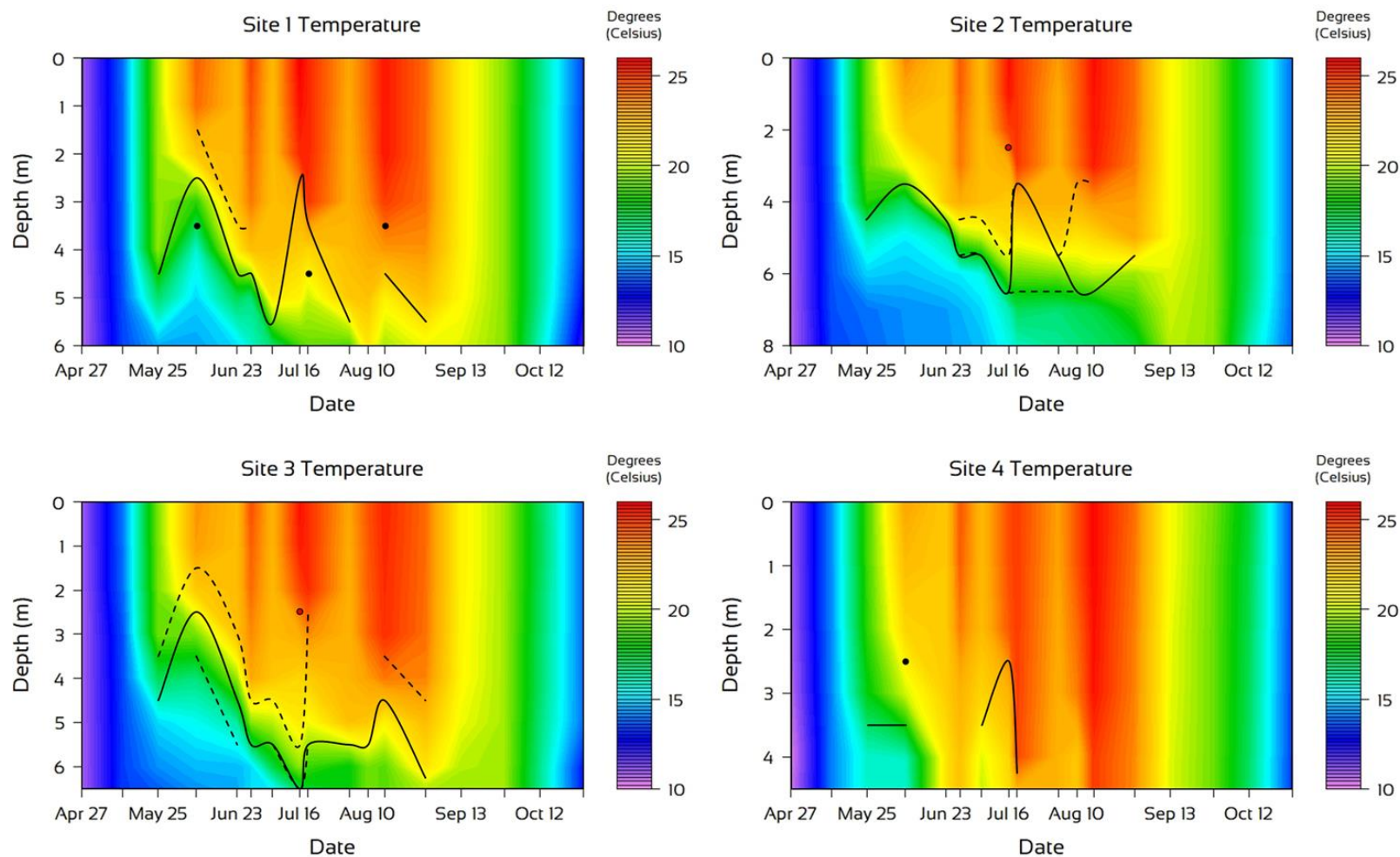


Figure 3. Isopleth plots of temperature at the NB (Site 1), CL (Site 2), PF (Site 3) and SB (Site 4) sites on Bantam Lake for the 2021 season. The black dashed lines and black dots represent the upper and/or lower metalimnetic boundaries. The solid black line represents the location of the thermocline. The red dot on the CL and PF isopleths represents a second thermocline observed on at those two sites on July 16th.

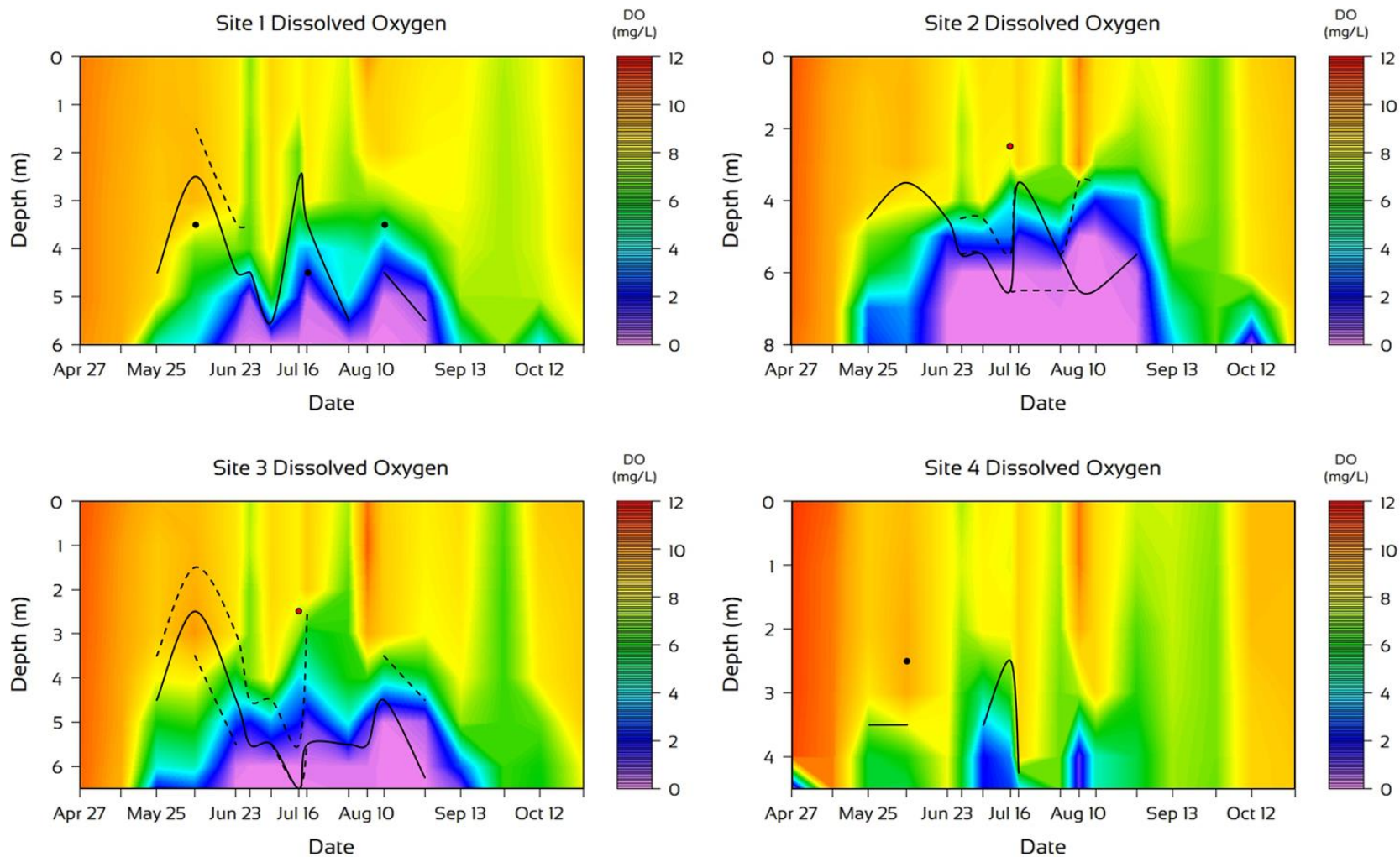


Figure 4. Isopleth plots of dissolved oxygen at the NB (Site 1), CL (Site 2), PF (Site 3) and SB (Site 4) sites on Bantam Lake for the 2021 season. The black dashed lines and black dots represent the upper and/or lower metalimnetic boundaries. The solid black line represents the location of the thermocline. The red dot on the CL and PF isopleths represents a second thermocline observed on at those two sites on July 16th.

Following August 16<sup>th</sup> and for the remainder of the season, temperatures in surface strata decreased and the water column mixed. August 31<sup>st</sup> was the date of the last sampling event when the lake was stratified at any site. It was also the last time oxygen levels <1mg/L were detected except at the PF site when the last day was September 13<sup>th</sup>.

## TROPHIC DATA

Much of the collected data were used to assess the trophic state of Bantam Lake. A lake's trophic state is a determination of the level of productivity the lake supports by assessing the variables that limit or are related to algal productivity, e.g., nutrient concentrations, Secchi transparency, chlorophyll-*a* concentrations, etc. Lakes supporting very little productivity are typically clear and are called oligotrophic; lakes supporting high levels of productivity are more turbid and are termed eutrophic or highly eutrophic. It is generally those eutrophic or highly eutrophic lakes that experience algal blooms. Table 1 lists the criteria often used to categorize the trophic state of a lake.

Table 2. Trophic classification criteria used by the Connecticut Experimental Agricultural Station (Frink and Norvell, 1984) and the CT DEP (1991) to assess the trophic status of Connecticut lakes. The categories range from oligotrophic or least productive to highly eutrophic or most productive.

Trophic Category	Total Phosphorus (µg / L)	Total Nitrogen (µg / L)	Summer Chlorophyll- <i>a</i> (µg / L)	Summer Secchi Disk Transparency (m)
Oligotrophic	0 - 10	0 - 200	0 - 2	>6
Early Mesotrophic	10 - 15	200 - 300	2 - 5	4 - 6
Mesotrophic	15 - 25	300 - 500	5 - 10	3 - 4
Late Mesotrophic	25 - 30	500 - 600	10 - 15	2 - 3
Eutrophic	30 - 50	600 - 1000	15 - 30	1 - 2
Highly Eutrophic	> 50	> 1000	> 30	0 - 1

## Chlorophyll-*a*

Chlorophyll-*a* is the primary photosynthetic pigment common to all freshwater algae, including cyanobacteria, and is used as a surrogate measurement for algal biovolume in lake water. Integrated samples from the top three meters of the water column, where light energy required for photosynthesis is greatest, were analyzed.



Individual chlorophyll-*a* concentrations spanned oligotrophic (NB, May 25<sup>th</sup>) to eutrophic (both NB and CL sites, September 13<sup>th</sup>; CL, October 12<sup>th</sup>) conditions. Summer month averages (July – September) at NB and CL were 10.9 and 20.1 µg/L, respectively, and representative of late-mesotrophic productivity. Respective season averages were 7.3 and 8.7µg/L and representative of mesotrophic productivity.

Chlorophyll-*a* levels were slightly elevated on April 27<sup>th</sup> and lowest at both sites on May 25<sup>th</sup> and June 23<sup>rd</sup> (Fig. 5). Concentrations modestly increased by July 19<sup>th</sup> and August 16<sup>th</sup> before a threefold increase by September 13<sup>th</sup>. Concentrations decreased by October 12<sup>th</sup> at the NB Site, but remained elevated at the CL Site.

It should be noted that chlorophyll-*a* data were representative of the concentrations throughout the top three meters of the water column, i.e., the average of all strata from the surface to 3m of depth. It is conceivable that a particular stratum within the top three meters had a higher concentration than others. For example, if much of the cyanobacteria community was positively buoyant and formed a surface scum then the highest concentration within the top 3m of the water column might be within the top 10cm of the water column.

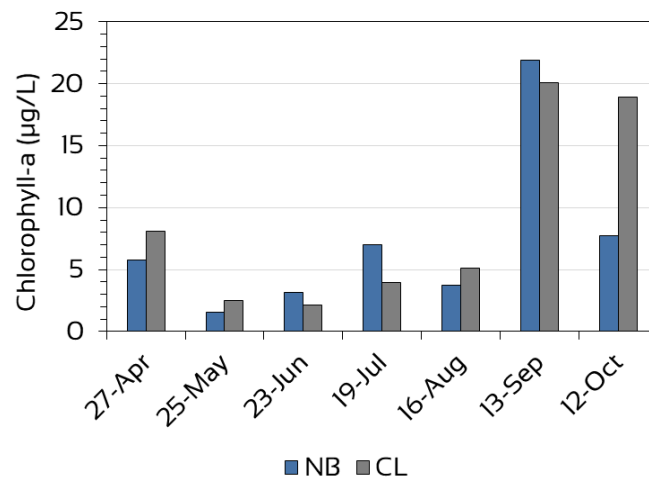


Figure 5. Chlorophyll-*a* concentrations measured at the North Bay (NB) and Center Lake (CL) sites on Bantam Lake in 2021.

### *Secchi Transparency and Compensation Depth*

Secchi disk transparency is a measure of how much light is transmitted through the water column. That transmission is influenced by a number of variables including the quantity of inorganic and organic particulate material in the water column that absorbs or reflects light. In the open water environment, Secchi disk transparency is inversely related to algal productivity.

Light in lakes is important for several reasons including its impact on open water photosynthesis and algal productivity. As light diminishes with depth, so too does maximum photosynthetic potential. Photosynthesis decreases with depth and there is a depth where oxygen produced from algal photosynthesis is equaled to the oxygen consumed via algal cellular respiration. That is referred to as the compensation point or compensation depth; it is estimated by multiplying the Secchi disk transparency by two.

Secchi disk transparency was measured 17 times at each site between April 27<sup>th</sup> and October 28<sup>th</sup>. Nine of those events were within the summer season (July – September). During that time, site averages were 1.91m at NB, 1.85m at CL, 1.77m at PF, and 1.74m at SB, and were not significantly different from each other ( $p>0.05$ ). The lake average was 1.81m and it, and summer site averages, were characteristic of eutrophic productivity.

The season site averages were 2.37m at NB, 2.34m at CL, 2.27m at PF, and 2.09m at SB, and not significantly different from each other ( $p>0.05$ ). The lake average for the season was 2.27m. All season site averages and the lake average were characteristic of late-mesotrophic productivity. The differences in the two sets of averages was due to the mesotrophic to late-mesotrophic Secchi transparencies measured at all sites between April 27<sup>th</sup> and July 6<sup>th</sup>. Average Secchi transparency decreased precipitously from 3.61m on June 23<sup>rd</sup> to 1.87m on July 16<sup>th</sup> (Fig. 6).

Compensation depths were calculated and are discussed below.

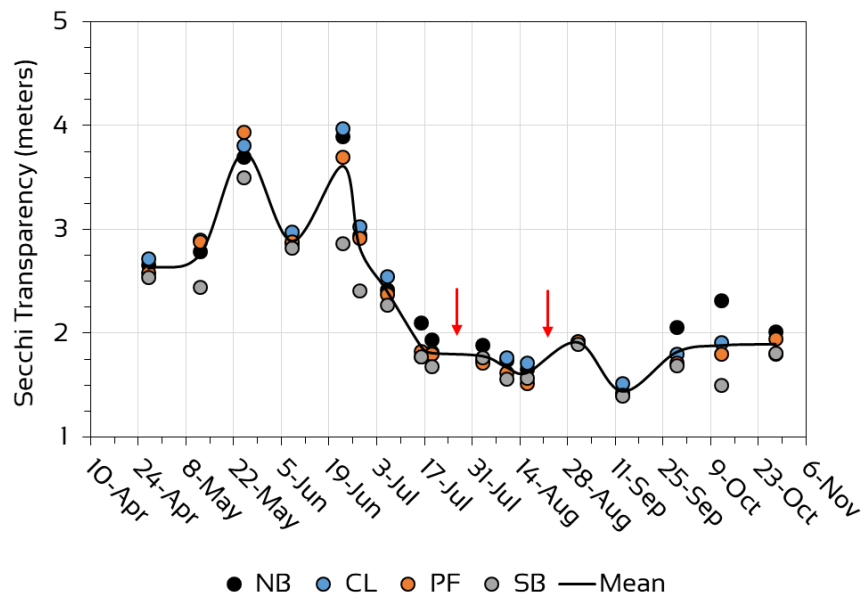


Figure 6. Secchi disk transparency measurements at the North Bay (NB), Center Lake (CL), Point Folly (PF), and South Bay (SB) sites in 2021. The black line connects the average (mean) Secchi transparencies of each day it was measured. The red arrows represent the approximate dates of the 2021 copper sulfate treatments of July 29<sup>th</sup> and August 24<sup>th</sup>.

## Total Phosphorus

Algae and cyanobacteria require a variety of macro and micronutrients. The nutrient that is least available in proportion to algal requirements is termed the *limiting nutrient*; in freshwater systems, that nutrient is usually phosphorus. It is the *limiting nutrient* because the amount of available phosphorus will limit the amount of algal growth in the system. In most Limnological studies, total phosphorus is measured, which is the sum of particulate and dissolved forms of phosphorus.

Epilimnetic and metalimnetic total phosphorus concentrations were similar at each site on each date throughout the season. Average epilimnetic concentrations were 22.1 and 25.0  $\mu\text{g/L}$  at the NB and CL sites, respectively. Average metalimnetic concentrations were 25.1 and 24.7  $\mu\text{g/L}$ , respectively. Averages were characteristic of mesotrophic productivity (Table 3). Concentrations at the NB site trended down from April 27<sup>th</sup> through June 23<sup>rd</sup> then increased to their maximum levels through August 16<sup>th</sup>. At the CL site, concentrations increased from April 27<sup>th</sup> through August 16<sup>th</sup>.

Total phosphorus concentrations on September 13<sup>th</sup> were greatly reduced at both sites, but especially at the CL site (Fig. 7). Epilimnetic and metalimnetic concentrations at both sites increased by October 12<sup>th</sup> and were all measured between 25 and 28  $\mu\text{g/L}$ .

Average hypolimnetic concentrations were 46 and 110  $\mu\text{g/L}$  at the NB and CL sites, respectively. These were capable of supporting eutrophic to highly-eutrophic algal productivity. Hypolimnetic concentrations were generally similar to concentrations in the other strata from April 27<sup>th</sup> through June 23<sup>rd</sup> (Fig. 7). Concentrations increased at

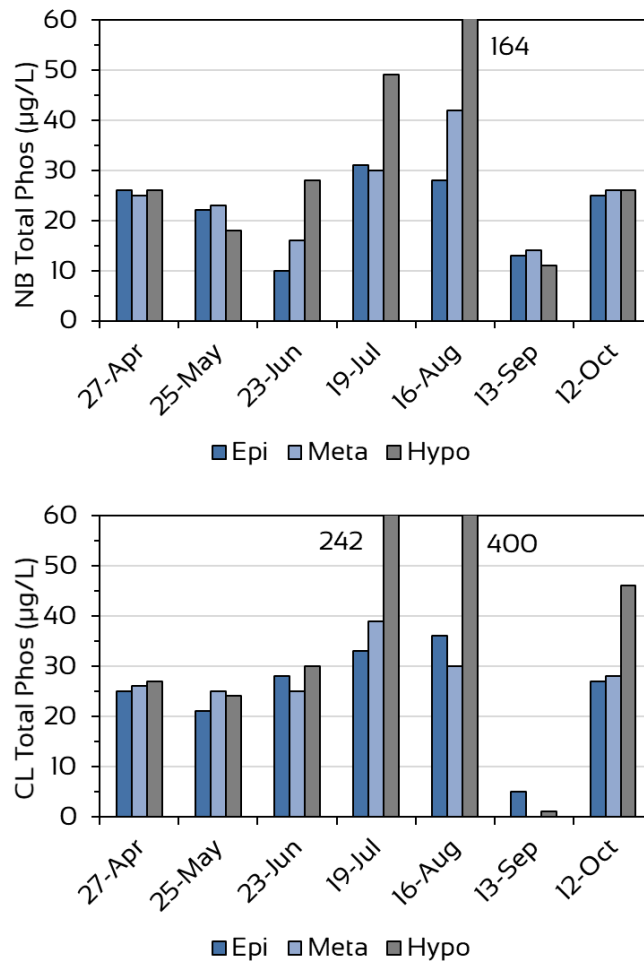


Figure 7. Total phosphorus concentrations in the epilimnion (Epi), metalimnion (Meta), and hypolimnion (Hypo) at the North Bay Site (top), and Center Lake Site (bottom) of Bantam Lake in 2021.



both sites by July 19<sup>th</sup> then reached their maximums of 164 and 400µg/L at the NB and CL sites, respectively, by August 16<sup>th</sup>. Season hypolimnetic minimums were measured on September 13<sup>th</sup> as they were at the other strata, and increased by October 12<sup>th</sup> to levels of the other strata at the NB site, and notably above epilimnetic and metalimnetic levels at the CL site (Fig 7).

### *Total Nitrogen*

Nitrogen is typically the second most limiting nutrient for algae growth in freshwater systems. It can be present in several forms in lake water. Ammonia – a reduced form of nitrogen – is important because it can affect the productivity, diversity, and dynamics of the algal and plant communities. Ammonia can be indicative of internal nutrient loading since bacteria will utilize other forms of nitrogen (e.g., nitrite and nitrate) in lieu of oxygen for cellular respiration under anoxic conditions, resulting in ammonia enrichment of the hypolimnion.

Total Kjeldahl nitrogen (TKN) is a measure of the reduced forms of nitrogen (including ammonia) and total organic proteins in the water column. Since TKN accounts for biologically derived nitrogen-rich proteins in the water column, it is useful in assessing the productivity of the lentic system. Nitrate and nitrite are often below detectable levels in natural systems because they are quickly cycled by bacteria and aquatic plants. Total nitrogen is the sum of TKN, nitrate, and nitrite; since the latter two are often below detectable limits, TKN levels are often similar or equal to total nitrogen levels.

Nitrogen constituents were analyzed in samples collected at one meter below the surface, at approximately 0.5m from the bottom, and at the thermocline during each sampling event. Due to a change in laboratory analyst in October, a higher minimum detection limit was used for TKN analyses for the October 12<sup>th</sup> samples. The detection limit was higher than the concentrations found in the samples, and sample concentrations were reported as <0.5mg/L. Those data are being excluded from our assessment.

Season average epilimnetic total nitrogen was 457 and 460µg/L at the NB and CL sites, respectively. Average metalimnetic concentrations were 491 and 504µg/L, respectively. All averages were within the range of mesotrophic algal productivity. All sample concentrations were <400µg/L from April 27<sup>th</sup> through June 23<sup>rd</sup> with the exception of the 466µg/L in the metalimnion of the CL site on June 23<sup>rd</sup>. The May 25<sup>th</sup> levels were the lowest of the season at these strata (Fig. 8). Concentration increased after June 23<sup>rd</sup> and reached their maximums in the epilimnion on August 16<sup>th</sup> of 715µg/L and 682µg/L at the NB and CL sites, respectively. Concentration in the metalimnion reached their respective maximums of 752 and 744µg/L on September 13<sup>th</sup>.

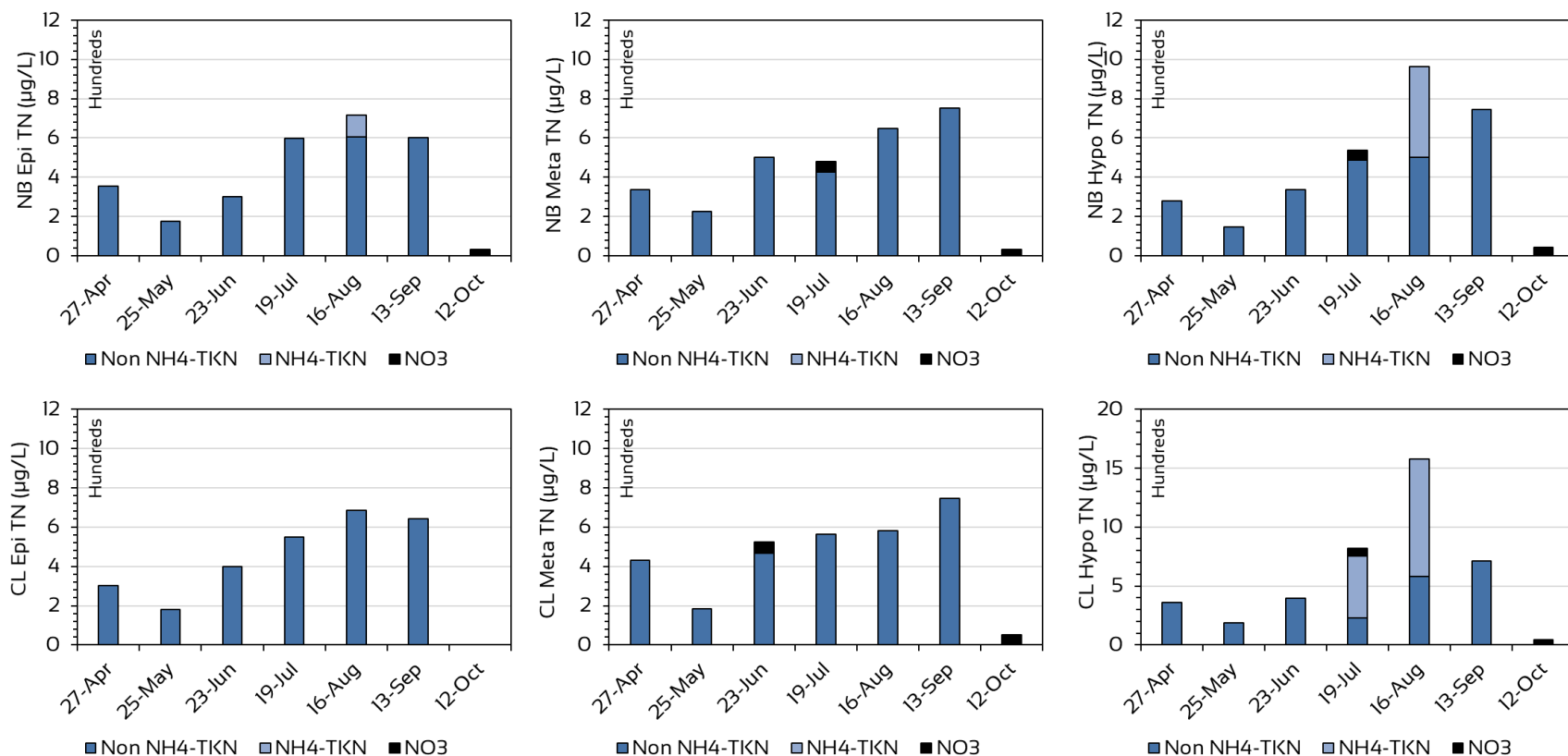


Figure 8. Total nitrogen concentrations in the epilimnion (Epi; left column), metalimnion (Meta; middle column), and hypolimnion (Hypo; right column) of the North Bay (NB; top row) and Center Lake (CL; bottom row) sites of Bantam Lake in 2021. Total nitrogen has been displayed in its separate constituents – total Kjeldahl nitrogen (TKN) that is not ammonia (Non-NH4 TKN), the ammonia component of TKN (NH4-TKN), and nitrate (NO3).

Within the epilimnetic and metalimnetic strata samples, ammonia was only detected at a concentration of 108µg/L in the epilimnetic sample on August 16<sup>th</sup> from the NB site. Nitrate was slightly more common in samples; and when detected, concentrations were between 30 and 60µg/L (Fig. 8).

Season average hypolimnetic total nitrogen concentrations were 501 and 675µg/L at the NB and CL sites, respectively and supportive of late-mesotrophic and eutrophic productivity. Hypolimnetic concentrations were similar to epilimnetic concentrations from April 27<sup>th</sup> to July 19<sup>th</sup> at the NB site and from April 27<sup>th</sup> to June 23<sup>rd</sup> at the CL site. Hypolimnetic concentrations diverged from epilimnetic concentrations once ammonia concentrations were detected (i.e., by July 19<sup>th</sup> at the CL and by August 16<sup>th</sup> at the NB site). Hypolimnetic season maxima were 961µg/L at the NB site and 1,575µg/L at the CL site. Both were from the August 16<sup>th</sup> samples. September 13<sup>th</sup> concentration decreased some, but were still elevated compared to early season levels.

### *Redfield Ratios*

Limnologists frequently use the Redfield ratio of 16 (16:1 nitrogen to phosphorus) to determine whether nitrogen or phosphorus is limiting in a freshwater system (Redfield 1958). The ratio is molar-based and when converted to mass, 7.2µg/L is the threshold. Values lower than the aforementioned threshold are indicative of nitrogen limitation while ratios above 7.2µg/L indicate phosphorus limitations. Nitrogen limitation favors cyanobacteria productivity due to the ability of some cyanobacteria to harvest elemental nitrogen dissolved into the water from the atmosphere, aka nitrogen fixation. Other algae taxa do not possess this ability.

Redfield ratios were determined for all strata where nutrient data was available, i.e., April 27<sup>th</sup> through September 13<sup>th</sup>. Most of the ratios for epilimnetic and metalimnetic samples were between 12 and 30. Exceptions occurred on May 25<sup>th</sup> and September 13<sup>th</sup>. On May 25<sup>th</sup>, ratios at the two sites and the two strata were between 7 and 10. On September 13<sup>th</sup>, when the lowest total phosphorus levels were measured, ratios were 46 and 54 in the epilimnion and metalimnion of the NB site, and 129 in the epilimnion of the CL site. No ratio was determined in the CL metalimnion on September 13<sup>th</sup> since total phosphorus was below detectable limits.

### **ALGAE AND CYANOBACTERIA DYNAMICS**

Much of the focus of lake management at Bantam Lake is the monitoring and treating of the seasonal cyanobacteria growth and reporting those activities to the community (BLPA 2021). In 2021, copper sulfate treatments took place at Bantam Lake on July 29<sup>th</sup> and August 24<sup>th</sup> to manage cyanobacteria growth. Biweekly monitoring of the cyanobacteria in Bantam Lake started on April 27<sup>th</sup> and concluded on October 28<sup>th</sup>.



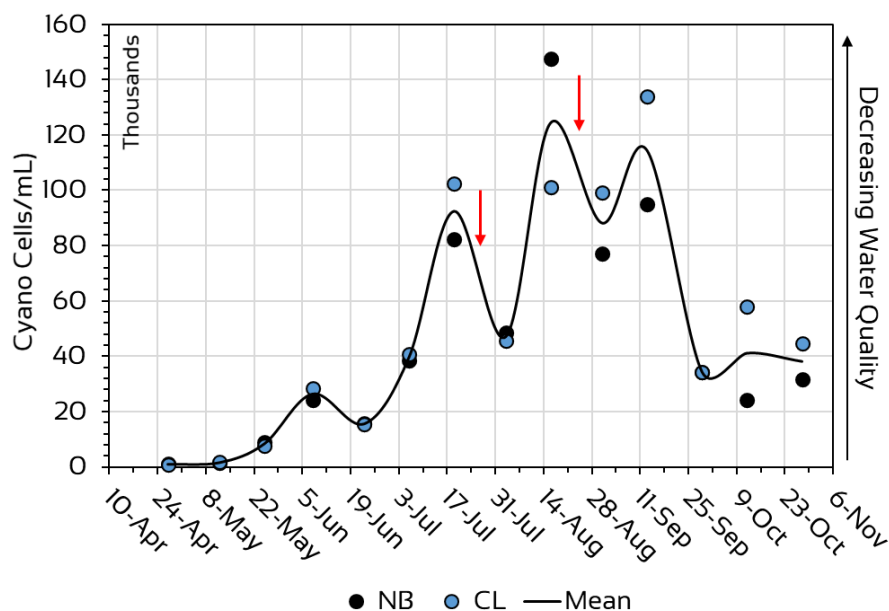


Figure 9. Cyanobacteria cell concentrations at the North Bay (NB) and Center Lake (CL) sites in 2021. The black line connects the average (mean) concentration for each sampling day. The red arrows represent the approximate dates of the 2021 copper sulfate treatments of July 29th and August 24th.

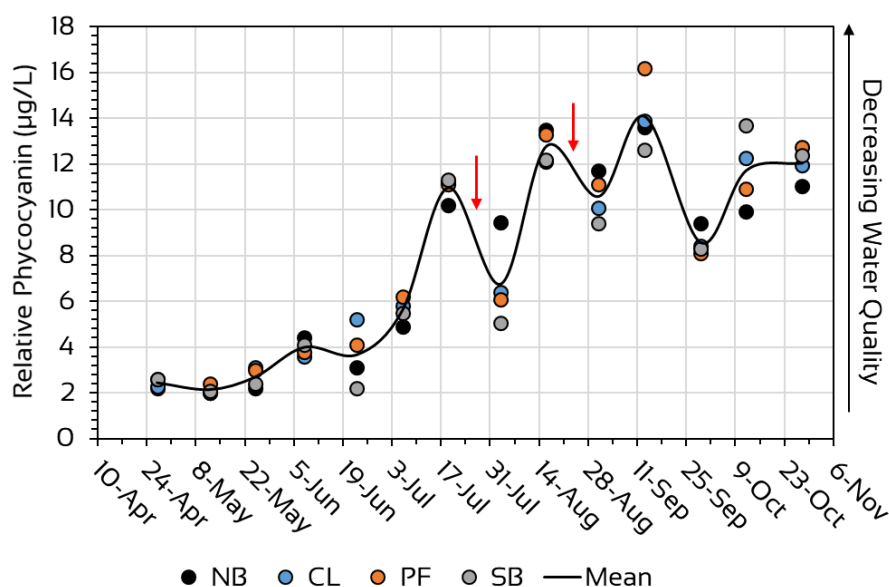


Figure 10. Relative phycocyanin concentrations at the North Bay (NB), Center Lake (CL), Point Folly (PF), and South Bay (SB) sites in 2021. The black line connects the average (mean) concentration for each day. The red arrows represent the approximate dates of the 2021 copper sulfate treatments of July 29th and August 24th.

### *Cyanobacteria Cell Concentrations and Relative Biomass*

Cyanobacteria cell concentrations in the first four-weeks of the season were <2,000 cells/mL (Fig. 9) and comprised  $\leq 30\%$  of the total algae cell concentrations. Average, cyanobacteria cell concentrations increased exponentially between May 12<sup>th</sup> and August 16<sup>th</sup> (Fig. 9). By May 25<sup>th</sup> at the CL site, and by June 8<sup>th</sup> at the NB site, cyanobacteria comprised a minimum of 90% of all cells counted. That relative abundance was maintained at both sites for the balance of the season with the exception of the CL site on August 3<sup>rd</sup> when the cyanobacteria relative abundance was 89%.

During that 14-week period of exponential increase in cell concentration, there was one two-week period – between June 19<sup>th</sup> and August 3<sup>rd</sup> – when a sizeable decrease in cell concentrations occurred at both sites (Fig. 8). That was likely the result of the July 29<sup>th</sup> copper sulfate treatment, the first of two treatments in 2021. However, by August 16<sup>th</sup> – approximately two weeks after the decrease – the maximum seasonal average was recorded with cyanobacteria cell concentrations measured at the NB and CL sites of 147,508 and 101,046 cells/mL, respectively (Fig. 9).

Subsequent to the maximum average cyanobacteria concentration, another decrease was observed. That decrease, measured in the August 31<sup>st</sup> samples, followed the second copper sulfate treatment that occurred on August 24<sup>th</sup>. Similar to the first treatment, average cyanobacteria cell concentration increased afterward to near the August 16<sup>th</sup> levels by September 13<sup>th</sup> (Fig. 9).

Cyanobacteria cell concentrations decreased to approximately 34,000 cells/mL by September 29<sup>th</sup>. From September 29<sup>th</sup> through October 28<sup>th</sup>, lake average concentrations remained relatively stable; individual site concentrations during that time fluctuated between approximately 24,000 and 58,000 cells /mL.

To supplement cyanobacteria cell concentrations, the photosynthetic pigment unique to the cyanobacteria – phycocyanin – in the top three meters of the water column was measured, averaged and plotted (Fig. 10). Relative phycocyanin was measured throughout the water column (see below) with a fluorimeter incorporated into the sensor array of the Eureka Manta II multiprobe. Fluorimeters work on the principal that a particular substance fluoresces at a specific wavelength when light of another wavelength is directed on that substance. The fluorimeter in AER's instrumentation emits a wavelength that interacts with phycocyanin. This sensor is not calibrated to known concentrations of phycocyanin so measurements are not quantitative; instead the measurements are relative to other measurements in the water column or to other sites. Measurements represent relative cyanobacteria biomass or biovolumes rather than cell concentrations.

The relationship between cyanobacteria cell concentrations and phycocyanin concentration was examined with linear regression. The averages of the top three meters of the water column of the NB and CL sites for each sampling event were regressed against the corresponding cyanobacteria cell concentrations and found to

be highly correlated ( $p < 0.001$ ). That correlation can be observed by comparing the biweekly cyanobacteria cell concentrations and relative phycocyanin concentrations (Figs. 9 & 10).

Changes in phycocyanin at all four sites paralleled the changes in cyanobacteria cell concentrations at the NB and CL sites during the course of the season, including the decreases following the two copper sulfate treatments (Fig. 10). There did appear to be some inconsistency in the last two samples (October 12<sup>th</sup> and October 28<sup>th</sup>) with relative phycocyanin cell concentrations not decreasing proportionally with cell concentrations. These dates corresponded with observations of some of the highest surface concentrations and a change in the dominant cyanobacteria genus.

### *Algal Taxa and Genera*

Fifty-nine algal taxa were identified unequally distributed among eight taxonomic groups (Table 3). The taxon with the greatest richness (numbers of genera) were the Chlorophyta (aka green algae) with 25 genera identified. Cyanobacteria, which was the taxon that was most abundant in the cell counts, was represented by 13 genera. Seven genera of Bacillariophyta (aka diatoms), five genera of Chrysophyta (aka golden algae), four genera of Pyrrophyta (aka dinoflagellates), and one genus each of Euglenophyta and Ochrophyta were observed in the 2021 season's samples.

Based on cell concentrations, early season samples were dominated by golden algae, particularly the colonial *Uroglenopsis spp.* that would continue to be observed throughout the season. Diatoms and cyanobacteria were the next most important taxa. Diatom genera included *Asterionella spp.*, *Aulocoseria spp.*, and *Fragilaria spp.* The filamentous cyanobacteria *Aphanizomenon spp.* was also important early and throughout the season. Other important early season cyanobacteria were *Aphanocapsa spp.* and *Woronichinia spp.* Cyanobacteria relative abundance was  $\leq 30\%$  at the two sites over the first two sampling periods.

By May 25<sup>th</sup>, cyanobacteria comprised 84.2 and 91.4% of total cells counted at the NB and CL sites, respectively. *Aphanizomenon spp.* and *Woronichinia spp.* continued to be important. Another filamentous cyanobacterium that increased in importance was *Dolichospermum spp.* (formerly *Anabaena spp.*); it too would be important for much of the season. *Uroglenopsis spp.* and *Dinobryon spp.* were the most abundant golden algae, which, as a taxonomic group, decreased in importance

From May 25<sup>th</sup> through August 30<sup>th</sup>, *Aphanizomenon spp.* was the dominant genus in the integrated samples. By September 29<sup>th</sup>, it had decreased in importance to 20.6 and 34.3% of all cells counted, but remained an important genus in samples. Other cyanobacteria genera that were counted at lower frequencies earlier in the season, became more important near the end of the season. These genera included *Dolichospermum spp.*, *Aphanocapsa spp.*, *Microcystis spp.*, *Planktothrix spp.*, *Pseudoanabaena*

*spp.*, and *Woronichinia spp.* Images of many of these and other genera discussed above, collected from Bantam Lake, are provided in Figures 11 and 12.

Table 3. Algal genera identified in from the plankton net samples and whole water samples collected at the NB and CL sites on Bantam Lake in 2021.

<b>Cyanobacteria</b>	<b>Chlorophyta</b>	<b>Chrysophyta</b>
<i>Aphanizomenon sp.</i>	<i>Anikistrodesmus sp.</i>	<i>Dinobryon sp.</i>
<i>Aphanocapsa sp.</i>	<i>Arthrodesmus sp.</i>	<i>Epipyxis sp.</i>
<i>Aphanothece sp.</i>	<i>Chlamydomonas sp.</i>	<i>Mallomonas sp.</i>
<i>Chroococcus sp.</i>	<i>Coelastrum sp.</i>	<i>Synura sp.</i>
<i>Coelosphaerium sp.</i>	<i>Crucigenia sp.</i>	<i>Uroglenopsis sp.</i>
<i>Cylindrospermopsis sp.</i>	<i>Dictyosphaerium sp.</i>	
<i>Dolichospermum sp.</i>	<i>Elakatothrix sp.</i>	<b>Pyrrhophyta</b>
<i>Gomphosphaeria</i>	<i>Eudorina sp.</i>	<i>Ceratium sp.</i>
<i>Microcystis sp.</i>	<i>Golenkinia sp.</i>	<i>Glenodinium sp.</i>
<i>Planktothrix sp.</i>	<i>Gloeocystis sp.</i>	<i>Gymnodinium sp.</i>
<i>Pseudoanabaena sp.</i>	<i>Gonium sp.</i>	<i>Peridinium sp.</i>
<i>Snowella sp.</i>	<i>Micractinium sp.</i>	
<i>Woronichinia sp.</i>	<i>Mougeotia sp.</i>	<b>Euglenophyta</b>
	<i>Nephrocytium sp.</i>	<i>Euglena sp.</i>
<b>Bacillariophyta</b>	<i>Oocystis sp.</i>	<i>Phacus sp.</i>
<i>Asterionella sp.</i>	<i>Padorina sp.</i>	<i>Trachelomonas sp.</i>
<i>Aulocoseria sp.</i>	<i>Pediastrum sp.</i>	
<i>Cyclotella sp.</i>	<i>Quadrigula sp.</i>	<b>Cryptophyta</b>
<i>Fragilaria sp.</i>	<i>Scenedesmus sp.</i>	<i>Cryptomonas sp.</i>
<i>Stephanodiscus sp.</i>	<i>Schroederia sp.</i>	
<i>Synedra sp.</i>	<i>Selenastrum sp.</i>	<b>Ochrophyta</b>
<i>Tabellaria sp.</i>	<i>Sphaerocystis sp.</i>	<i>Stichogloea sp.</i>
	<i>Staurostrum sp.</i>	
	<i>Tetraedron sp.</i>	
	<i>Ulothrix sp.</i>	



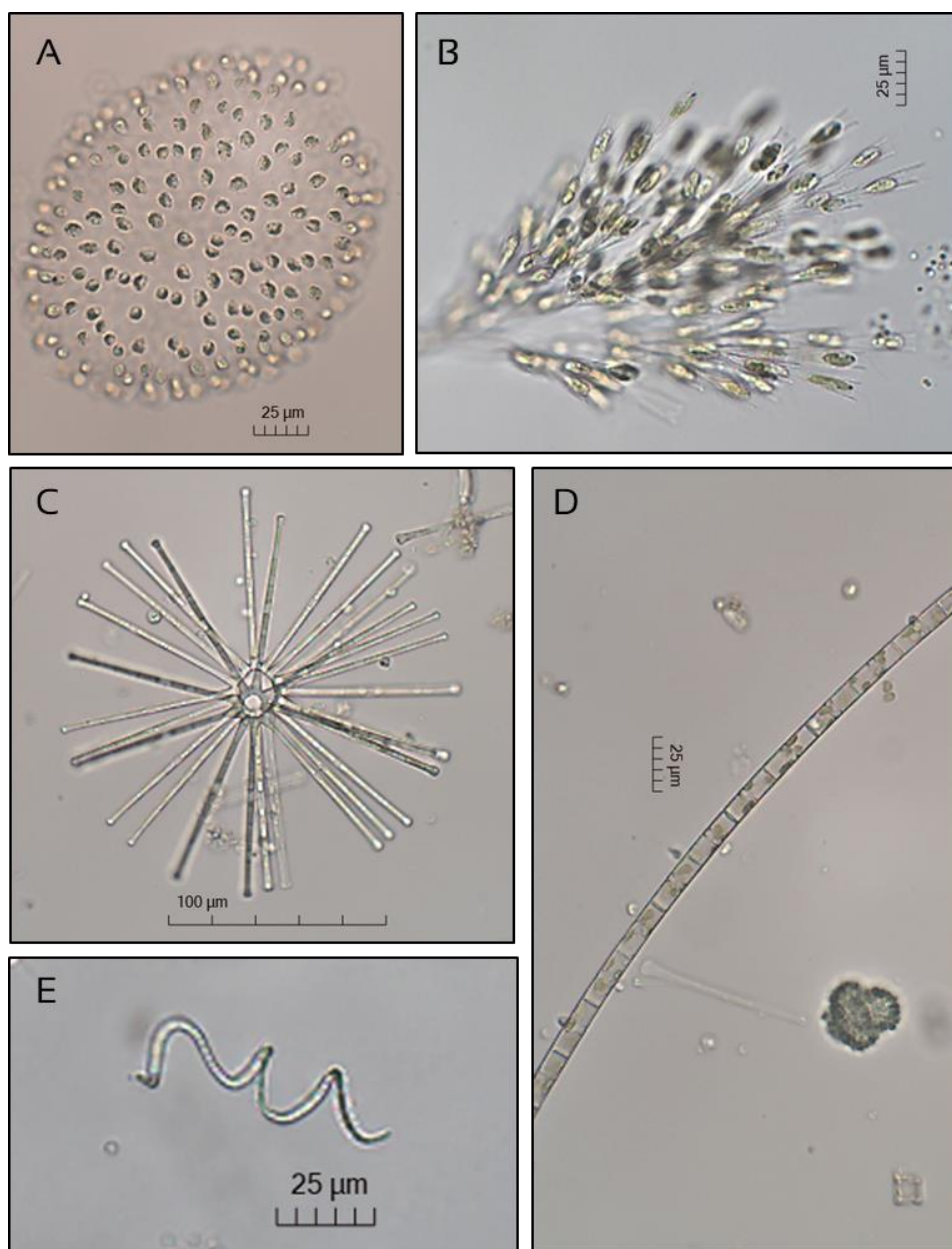


Figure 11. Algal specimens collected from Bantam Lake in 2021. Golden algae genera *Uroglenopsis* spp. (A) and *Dinobryon* spp. (B); diatom genera *Asterionella* spp. (C) and *Aulocoseria* spp. (D); and the cyanobacteria *Cylandrospermopsis* spp.



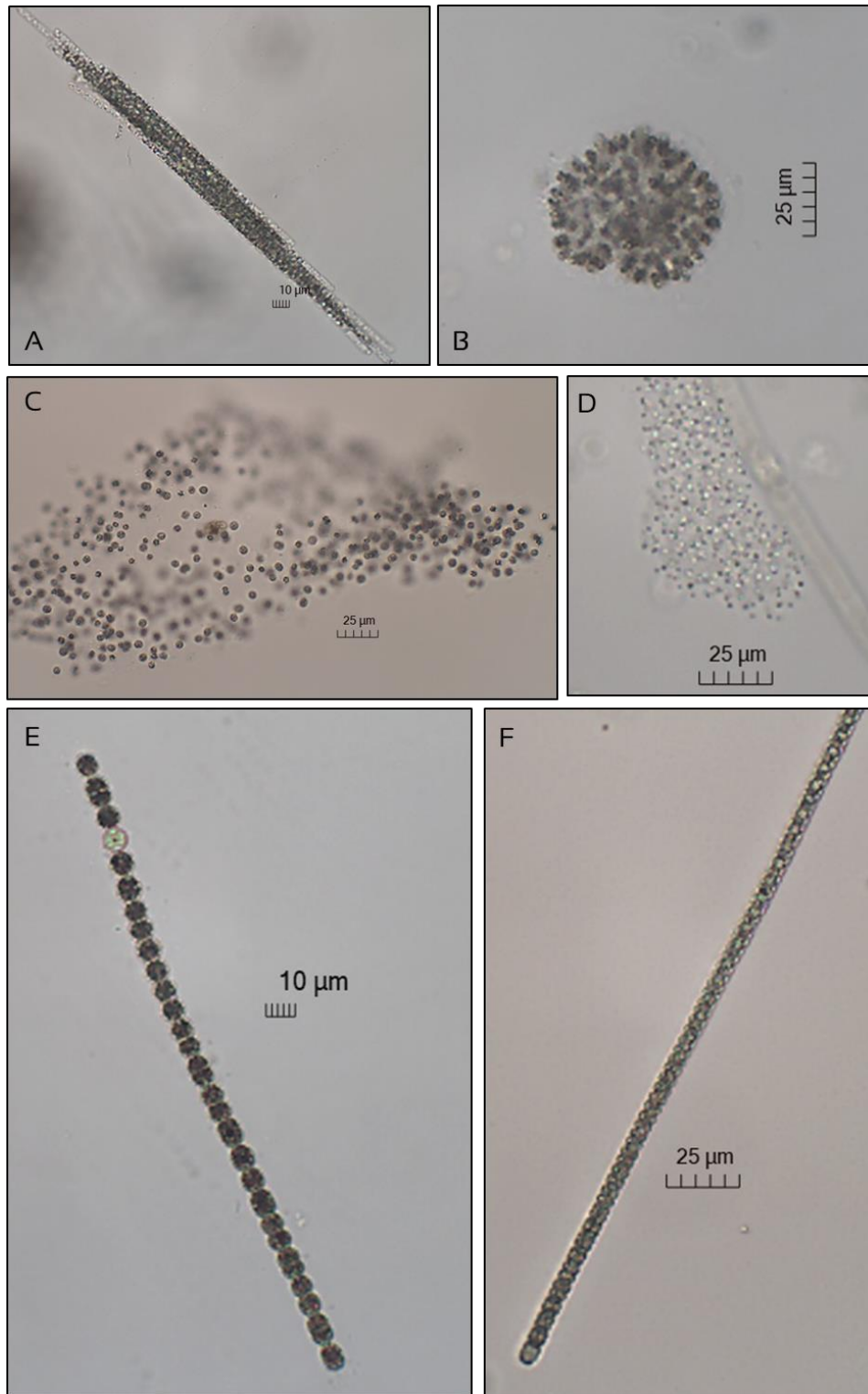


Figure 12. Specimens of cyanobacteria genera collected from Bantam Lake in 2021. A) a raft of *Aphanizomenon* spp., B) *Woronichinia* spp., C) *Microcystis* spp., D) *Aphanocapsa* spp., E) *Dolichospermum* spp., and F) *Planktothrix* spp.

One notable observation in the August 16<sup>th</sup> plankton net sample, but not in the whole water samples, was the small filamentous cyanobacterium *Cylindrospermopsis* spp. (Fig. 9). This was the first time AER had observed this genus at Bantam Lake.

### *Cyanobacteria Spatial and Temporal Distribution*

As noted earlier, relative phycocyanin concentrations were measured throughout the water column on each date that samples were collected for cyanobacteria cell counts. As performed with other data collected throughout the water column (e.g., temperature, dissolved oxygen), graphic representation of relative phycocyanin concentration across depths and dates were created using isopleth plots (Fig. 13).

In the *Cyanobacteria Cell Concentrations and Relative Biomass* section above, we reported on average conditions in the top three meters of the water column for each site across the season. Here, the differences within the water column are discussed over time.

Relative phycocyanin concentrations were uniformly low throughout the water columns of the four sites from April 27<sup>th</sup> through May 25<sup>th</sup>. By June 8<sup>th</sup>, distribution within the water column started to become less uniform with mid-depths exhibiting slightly higher phycocyanin concentrations than surface or bottom strata, with the exception of the NB site where surface concentrations were also slightly elevated (Fig. 13). Vertical distribution of phycocyanin varied from site to site on June 23<sup>rd</sup>. By July 6<sup>th</sup>, a trend of higher concentrations in depths above the upper metalimnetic boundary or above the thermocline at the NB, CL, and PF sites began to emerge (Fig. 13). At the SB site, concentrations tended to be more equally distributed vertically.

Differences between sites became more evident between July 19<sup>th</sup> and September 29<sup>th</sup>. For example, surface phycocyanin concentration at the NB site were consistently high during that period of time. The other sites had alternating periods of higher and lower concentrations in strata near the surface over that timeframe. Highest relative concentrations were observed in the top four meters of the PF site water column on September 13<sup>th</sup>. Season maxima for the NB and SB sites occurred on October 12; at the NB site the highest concentration was at 3m of depth, and at the SB site it was at 2m of depth.

On September 29<sup>th</sup>, all sites exhibited a decrease in relative phycocyanin concentration throughout the water column. Subsequently, concentrations increased throughout much of the water columns at the CL, PF, and SB sites. At the NB site, higher concentrations were largely limited to the 2 to 4m strata (Fig. 13).

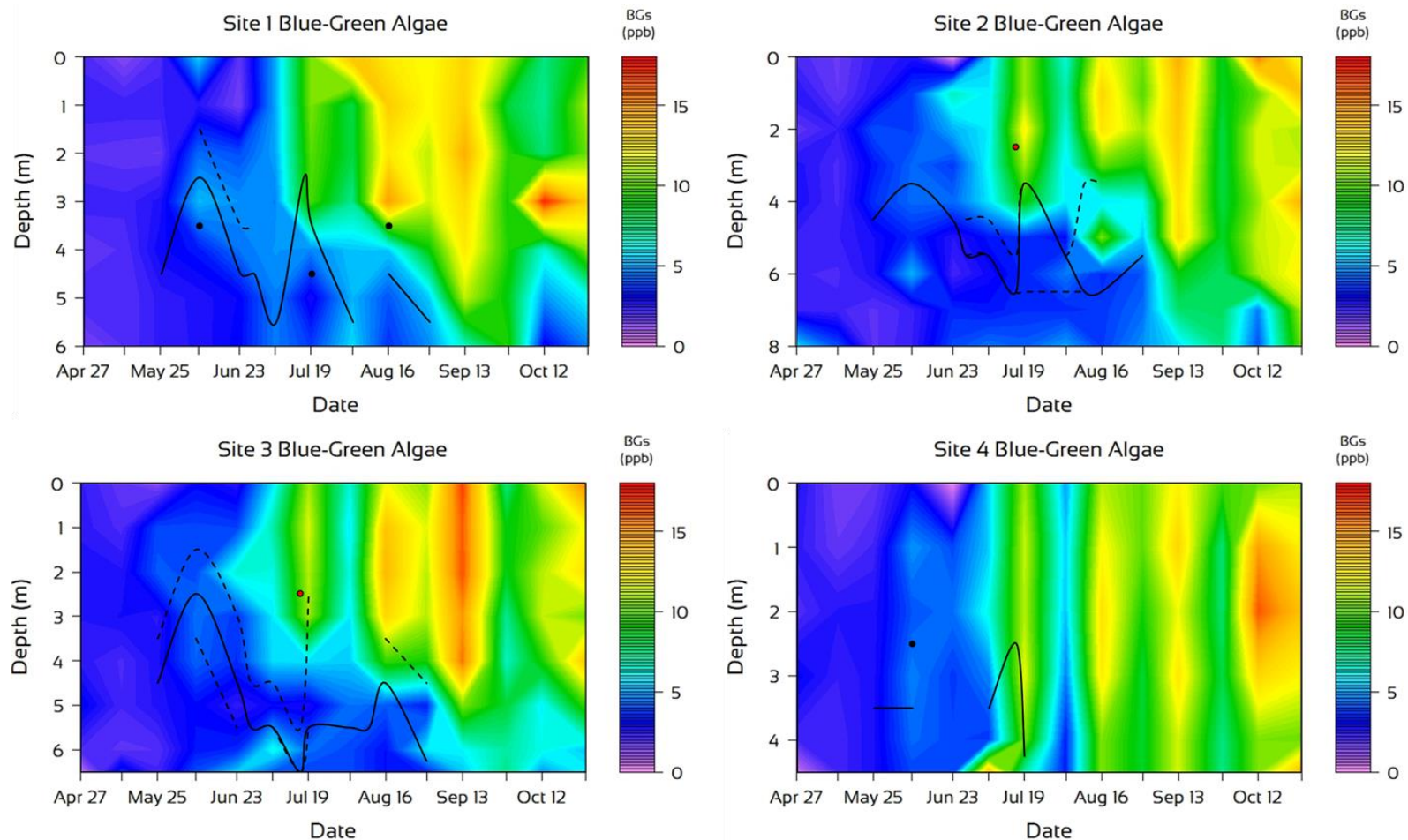


Figure 13. Isopleth plots of relative phycocyanin concentration at the NB (Site 1), CL (Site 2), PF (Site 3) and SB (Site 4) sites on Bantam Lake for the 2021 season. The black dashed lines and black dots represent the upper and/or lower metalimnetic boundaries. The solid black line represents the location of the thermocline. The red dot on the CL and PF isopleths represents a second thermocline observed on at those two sites on July 16<sup>th</sup>.

## Cyanotoxin Monitoring

The human and animal health risks associated with cyanobacteria are due to the toxins some genera are capable of synthesizing. There are at least nine different known toxins that are produced by the cyanobacteria. Several of those have numerous known congeners, e.g., Microcystin has 80 to 90 congeners (Cheung et. al. 2013, CT DPH & CT DEEP 2019, USEPA 2014, 2021). Microcystin is considered the most pervasive in freshwater systems and the Microcystin-LN congener is considered one of the most toxic of all the cyanotoxins.

Many of the cyanobacteria genera observed at Bantam Lake are considered toxigenic, i.e., some populations have synthesized toxins in the natural environment or in laboratory settings (CT DPH & CT DEEP 2019, Cheung et. al. 2013, USEPA 2020). In 2019, the BLPA engaged Dr. Edwin Wong in the Biology and Environmental Science Department at Western Connecticut State University to develop a program to monitor microcystin levels in waters samples collected by AER during biweekly visits. The program was continued in 2021.

The samples were integrations of the top three meters of the water columns and from the NB and CL sites. Microcystin is one of the most common of a number of cyanotoxins produced by Cyanobacteria. The State of Connecticut recommends using a threshold of 8µg/L, above which beach closure signage should remain deployed. Results of 2021 analyses are presented in Table 3. Despite high cyanobacteria cell concentrations and phycocyanin levels, Microcystin levels never exceeded 0.5µg/L.

Table 4. Microcystin concentrations in µg/L in samples collected at Bantam Lake in 2021.

Date	NB Site	CL Site
8-Jun	0.063	0
22-Jun	0.03	0.02
6-Jul	0.058	0.192
30-Jul	0.023	0.041
10-Aug	0.052	0.083
19-Aug	0.261	0.211
3-Sep	0.222	0.264
13-Sep	0.106	0.174
21-Sep	0.049	0.194
12-Oct	0.126	0.231
28-Oct	0.146	0.169

## BANTAM LAKE CHEMISTRY

Data on water chemistry not directly related to the trophic status of the lake are reported on below. These water quality characteristics can have indirect impacts on the biota inhabiting the lake. They also serve to detect changes in levels of stormwater-driven pollutant levels entering the lake, and the importance of internal loading of nutrients from lake sediments to the nutrient budget of the lake.

### *Specific Conductance*

Conductivity is a surrogate measurement for the ionized minerals, metals, and salts in the water. As such, it is also a measure of water's ability to conduct an electrical current. Data collections included measures of conductivity, which were measured in microsiemens per cm ( $\mu\text{S}/\text{cm}$ ). We report below on specific conductance, which is conductivity but standardized to a set water temperature ( $25^\circ\text{C}$ ). Temperature influences conductivity and – in the field – temperature varies with depth and date.

Specific conductance is an important metric in Limnological studies due to its ability to detect pollutants and/or nutrient loadings. Specific conductance can also have an influence on organisms that inhabit a lake or pond; particularly, algae. The composition of algal communities has been shown to be related, in part, to conductivity levels in lakes (e.g., Siver 1993, McMaster & Schindler 2005). As was done with temperature and oxygen profile data, specific conductance data have been displayed as an isopleth plots (Fig. 14).

Specific conductance was constant throughout the water column on April 27<sup>th</sup> and May 12<sup>th</sup> (prior to stratification) and averaged  $203\mu\text{S}/\text{cm}$  based on measures from all four sites and all depths on those two days. By May 25<sup>th</sup> and through June 6<sup>th</sup>, minor differences with depth were observed at the NB, CL, and PF sites with levels above the thermocline slightly higher than most levels below the thermocline. The exception was at the very bottom of the water column at the deeper CL and PF sites where the highest measurements were taken.

By June 23<sup>rd</sup>, the four-site epilimnetic average had increased to  $209\mu\text{S}/\text{cm}$  with the highest epilimnetic level of  $211\mu\text{S}/\text{cm}$  at the NB site, lowest level at the SB site at  $207\mu\text{S}/\text{cm}$ , and the CL/PF site levels of  $209\mu\text{S}/\text{cm}$ . The latter two sites also exhibited elevated levels ( $220$  and  $216\mu\text{S}/\text{cm}$ , respectively) at the bottom of the water column. A modest decrease in specific conductance was measured throughout the top five meters of the water column by July 19<sup>th</sup> through August 3<sup>rd</sup>, while levels at the bottom of the deeper CL and PF sites increased to  $264$  and  $238\mu\text{S}/\text{cm}$ . Hypolimnetic increases in specific conductance would continue at those two sites through August 31<sup>st</sup> when maximum levels of  $283$  and  $255\mu\text{S}/\text{cm}$ , respectively were reached. The epilimnetic average on August 31<sup>st</sup> had decreased to  $195\mu\text{S}/\text{cm}$ .

Notable changes in specific conductance occurred after August 31<sup>st</sup> (Fig. 14). First, specific conductance throughout the water column was generally uniform, and secondly, almost all measurements from September 13<sup>th</sup> through the end of the season were  $<170\mu\text{S}/\text{cm}$ . The exception was the NB site on September 13<sup>th</sup> when surface levels of  $171\mu\text{S}/\text{cm}$  increased with depth to  $174\mu\text{S}/\text{cm}$  at the bottom. By October 28<sup>th</sup>, the greatest specific conductance measurement from all four sites was  $164\mu\text{S}/\text{cm}$  measured in the top 4m of the NB water column.



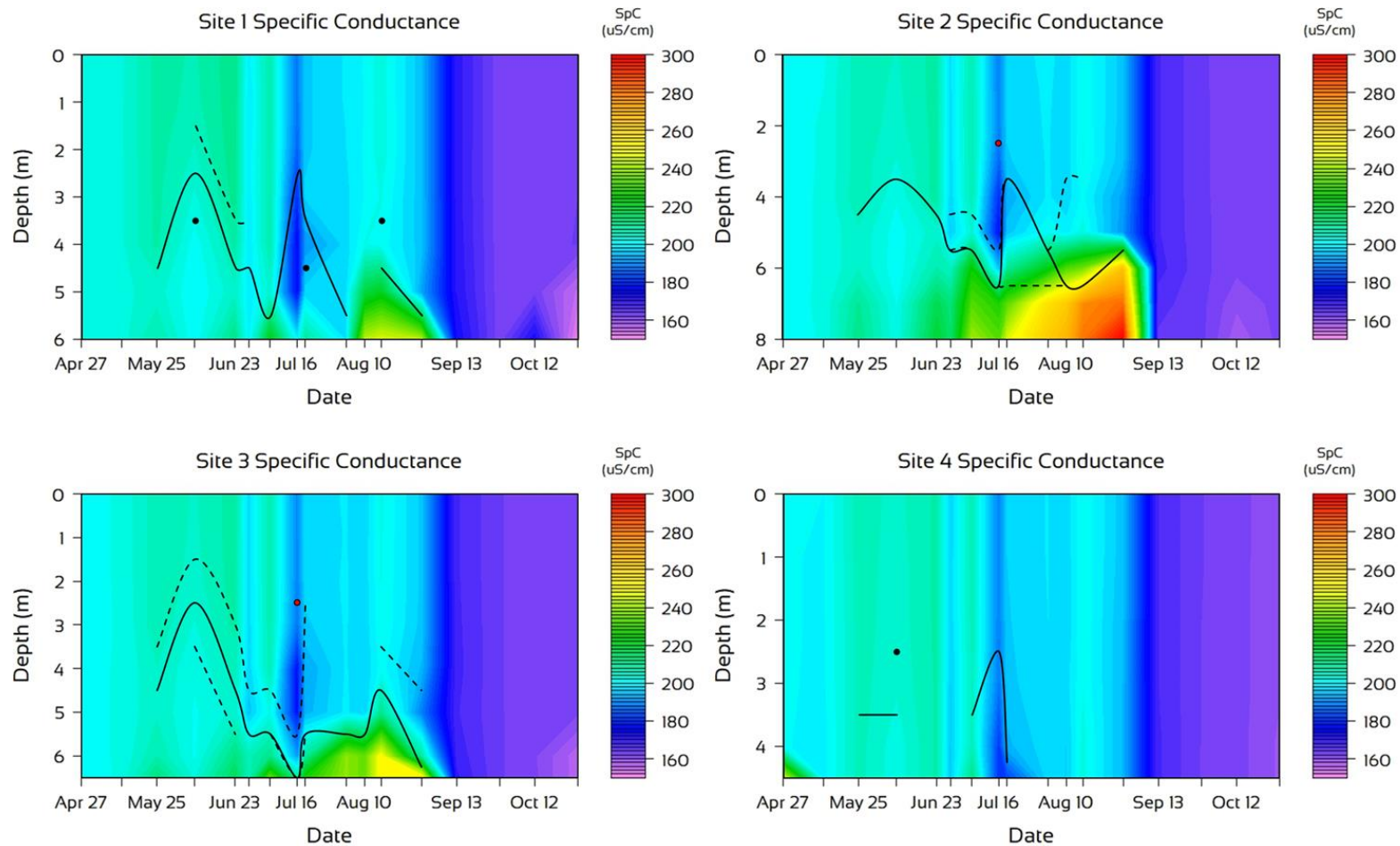


Figure 14. Isopleth plots of specific conductance at the NB (Site 1), CL (Site 2), PF (Site 3) and SB (Site 4) sites on Bantam Lake for the 2021 season. The black dashed lines and black dots represent the upper and/or lower metalimnetic boundaries. The solid black line represents the location of the thermocline. The red dot on the CL and PF isopleths represents a second thermocline observed on at those two sites on July 16th.

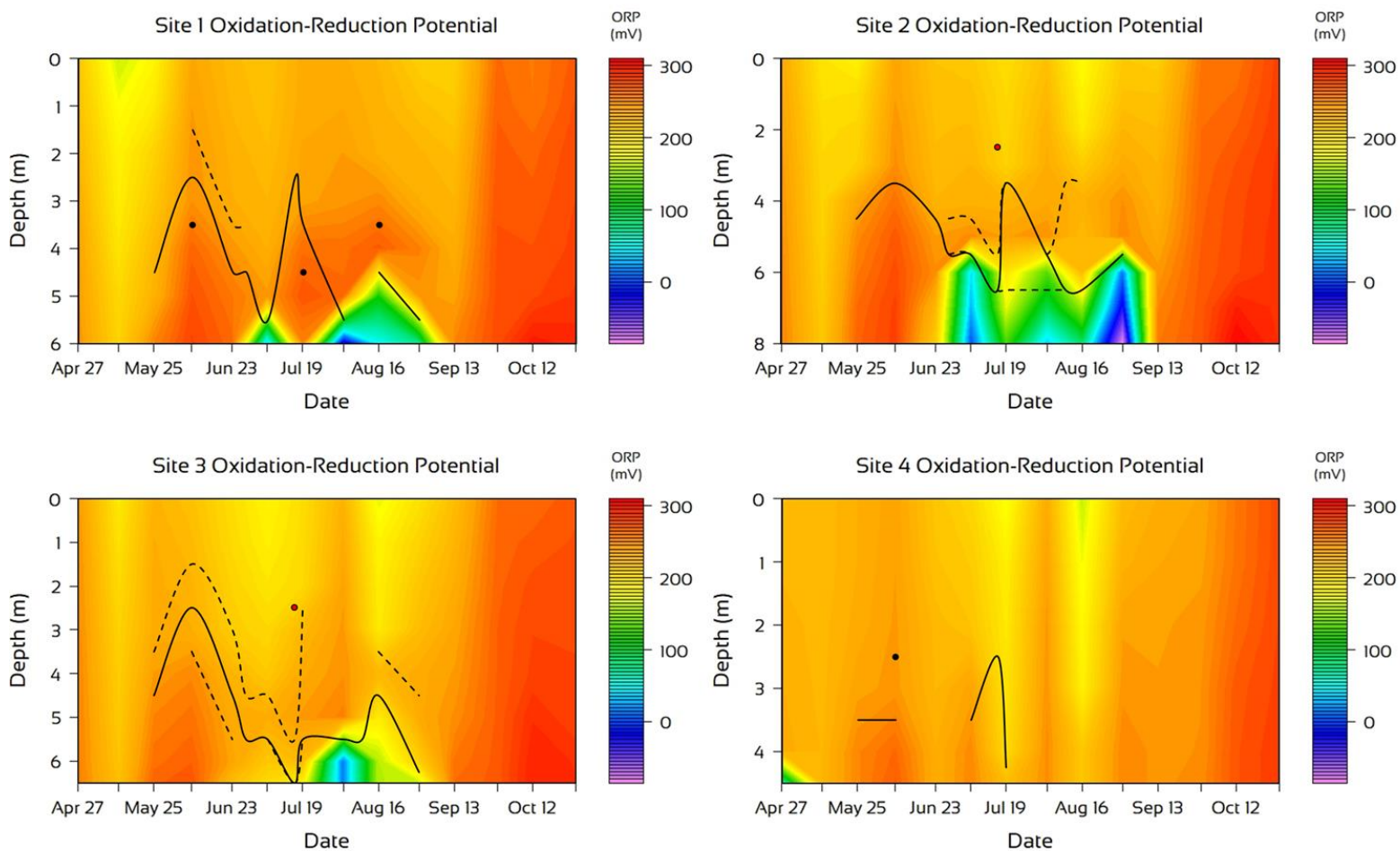


Figure 15. Isopleth plots of oxidation-reduction potential at the NB (Site 1), CL (Site 2), PF (Site 3) and SB (Site 4) sites on Bantam Lake for the 2021 season. The black dashed lines and black dots represent the upper and/or lower metalimnetic boundaries. The solid black line represents the location of the thermocline. The red dot on the CL and PF isopleths represents a second thermocline observed on at those two sites on July 16th.

### *Oxidation-Reduction Potential*

The oxidation-reduction potential (aka redox potential or ORP) in lakes refers to the oxidative or reductive state in a particular stratum of the water column; it can provide some insight as to whether phosphorus is changing from an insoluble particulate state in lake sediments to a soluble state that readily diffuses to overlying waters and available to lentic algae if mixed into the photic zone (i.e., where algae can harvest it for growth). When ORP is  $\geq 200$  millivolts (mV) phosphate remains bound to available iron; at ORP values of  $< 200$  mV, iron is reduced and the phosphate that is chemically bound to the iron becomes soluble (Søndergaard 2009). In some cases, a sudden mixing of phosphate-laden bottom waters to the upper reaches of the water column during a storm or wind event can trigger an algae bloom. ORP data collected at the four sites is presented as isopleth plots (Fig. 15).

Oxidation-reduction potentials in the epilimnion, or surface strata when the water column was mixed, were normally  $> 200$  mV with some exceptions including measurements on May 12<sup>th</sup> at the NB, CL, and PF sites, and on August 16<sup>th</sup> at the CL, PF, and SB sites. These were rarely below 180 mV, and never below 160 mV.

ORP below the thermocline was regularly  $< 200$  mV, especially at the NB, CL, and PF sites in July and August (Fig. 14). Only once was a measurement of  $< 200$  mV observed at the bottom of SB water column, which was 63 mV on April 27<sup>th</sup>. The first time low ORP was observed at the NB site, it was -32 mV at the 6 m stratum on July 6<sup>th</sup>. However, on July 19<sup>th</sup>, ORP at the 6 m stratum was 267 mV. Measurements of 78 to -30 mV were recorded at the NB site, and at the 6 m stratum during the August visits (Fig. 15). On August 16<sup>th</sup> an ORP of 115 mV was also recorded at the 5 m stratum.

At the PF site, the first low ORP reading was on July 19<sup>th</sup> at 6.5 m of depth and was 188 mV. On the following visit on August 3<sup>rd</sup>, 14 mV was recorded at the 6 and 6.5 m strata. The same strata increased to 159 mV by August 16<sup>th</sup>. By August 31<sup>st</sup>, the 6.5 m stratum was 164, but 212 mV at the 6 m stratum.

At the CL site, the deepest sampling site, July 6<sup>th</sup> ORP from the 6 to 8 m stratum decreased from 41 to 2 mV, respectively. On the following sampling date – July 19<sup>th</sup> – ORP decreased from 195 to 129 mV, within the same respective strata. Similar changes were observed on August 3<sup>rd</sup> but ORP was within a lower range, i.e., 134 to 95 mV. By August 16<sup>th</sup>, only the 7 and 8 m strata were  $< 200$  mV; a measurement of 152 mV was recorded at the 7 m stratum, and of 87 mV at the 8 m stratum. The last time low ORP measurements were recorded at the CL site, or any site, was August 31<sup>st</sup>. On that date at the CL site, between the 6 and 8 m strata, ORP decreased from 13 to -85 mV.



### *Base Cations and Chloride*

Base cation and anion concentrations are important in understanding natural influences (e.g., dissolved salts from bedrock geology) as well as anthropogenic influences in the watershed (e.g., road salts). In most lakes, the dominant base cations in lake waters are calcium ( $\text{Ca}^{2+}$ ), magnesium ( $\text{Mg}^{2+}$ ), sodium ( $\text{Na}^+$ ) and potassium ( $\text{K}^+$ ). Dominant anions include chloride ( $\text{Cl}^-$ ), sulfate ( $\text{SO}_4^{2-}$ ), and the alkalinity ions, i.e., carbonate ( $\text{CO}_3^{2-}$ ), and bicarbonate ( $\text{HCO}_3^-$ ). Those cations and anions are what collectively contribute to conductivity levels in lake water. The ratios of those ions and combinations of those ions can be diagnostic when compared to other lakes, and when compared to levels in the same lake over time.

Monthly base cations, chloride, and the alkalinity anion data was reported by the commercial laboratory based on their mass (mg/L). We report them based on their electrochemical equivalents (meq/L). The latter was calculated by dividing the measured mass of an ion by its equivalent weight. This provides a means of accounting for the ionic charge (positive or negative). Accounting for electric charge can be preferable when comparing ion levels to other electrochemical characteristics of lake water, e.g., specific conductance.

Sodium, followed by calcium, were the most abundant base cations, especially in samples collected from April 27<sup>th</sup> to July 13<sup>th</sup> (Fig. 15). Sodium was the most dynamic of the base cations with higher concentrations of 0.65 to 0.74 meq/L measured prior to September 9<sup>th</sup>, and a concentration of 0.52 meq/L on that date and October 19<sup>th</sup> at the NB and CL sites. Calcium concentrations were more conservative, with early season concentrations of 0.50 to 0.55 meq/L, mid-season levels of 0.60 to 0.65 meq/L, and 0.55 to 0.60 meq/L in September and October samples, respectively (Fig. 16). Magnesium was the most conservative of the detectable base cations, only ranging from 0.38 to 0.44 meq/L for the season at both sites. Potassium was reported as not detected and likely below the laboratory's minimum detectable limit in samples.

Seasonal trends in anions measured in samples were detected. Highest chloride concentrations of 0.93 to 0.96 meq/L were measured in samples collected from April 27<sup>th</sup> to June 17<sup>th</sup>. Concentrations decreased over time until those measured on September 9<sup>th</sup> and October 19<sup>th</sup> were between 0.58 to 0.61 meq/L (Fig. 16). Low alkalinity concentrations of 0.72 to 0.76 meq/L were measured in early season samples, and were generally between 0.76 and 0.92 meq for the balance of the season. The exception was the 1.28 meq/L measured at the NB site on August 11<sup>th</sup>, which appears anomalous.

The water samples from the two sites were, on average, charge balanced. When the anomalous alkalinity at NB site on August 11<sup>th</sup> was removed, the cation to anion ratio was 1.62 meq/L to 1.62 meq/L, but 1.62 meq/L to 1.69 meq/L when the data point was included. At the CL site, the ratio was 1.64 meq/L to 1.61 meq/L (Fig. 16).

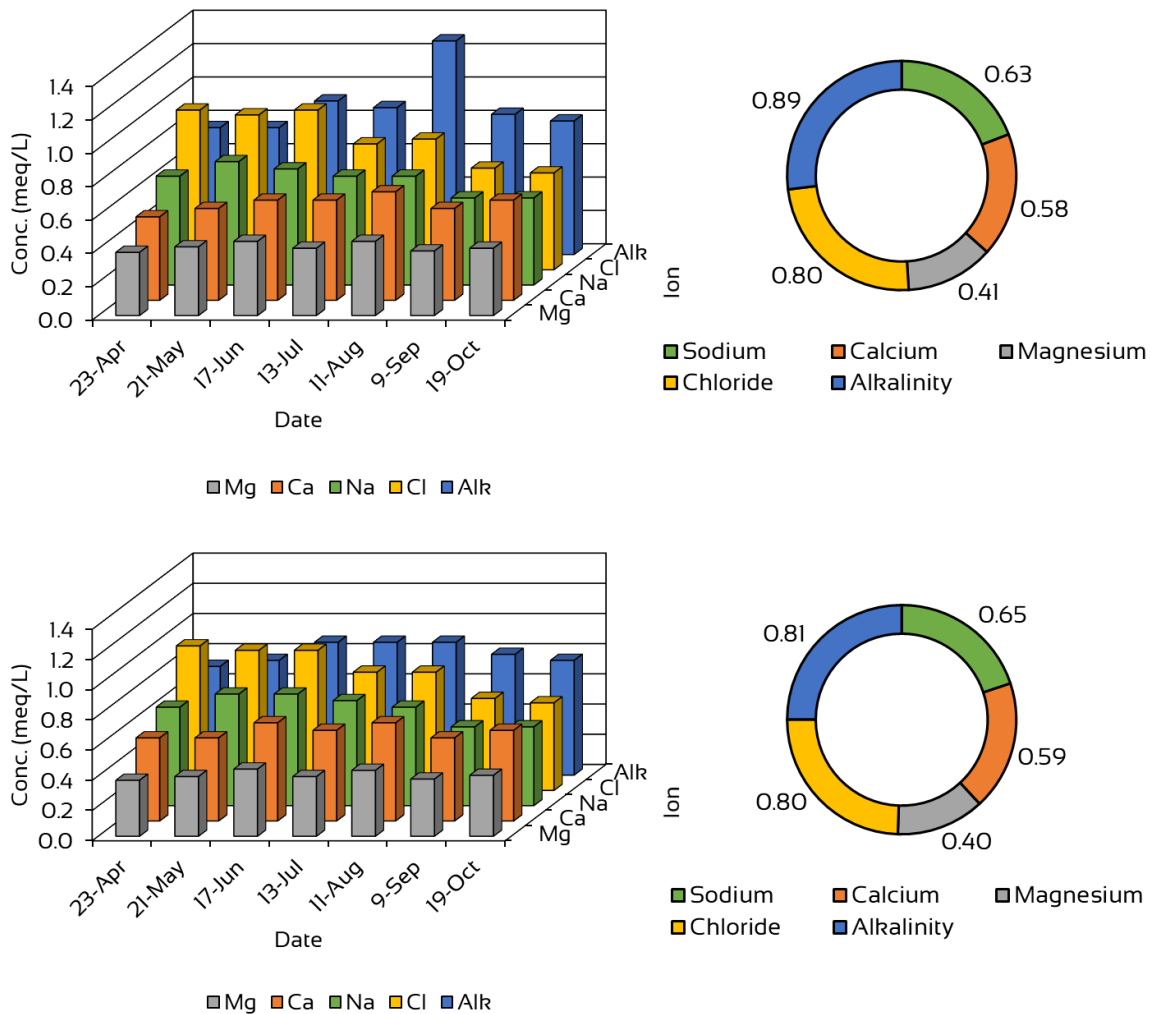


Figure 16. Concentrations of base cations and anions (left) and averages for the season (right) for the NB site (top) and CL site (bottom). Mg = magnesium; Ca = calcium; Na = sodium; Cl = chloride; and Alk = alkalinity anions. Conc. = concentration.

### Alkalinity and pH

Alkalinity is a measure of the water's calcium carbonate content and provides lake water its ability to neutralize acid (i.e., buffering capacity). Alkalinity of surface waters is largely influenced by local geology and other watershed characteristics. Bantam Lake lies in the Western Uplands geological region of Connecticut where bedrock is largely erosion resistance and surficial materials are glacial till (Canavan and Siver 1994). Alkalinity at the bottom of the water column can also be generated internally from the biologically mediated reduction of iron, manganese, and sulfate via cellular respiration in the anoxic lake sediments, and denitrification of nitrate to elemental nitrogen (Wetzel 2001).

For purposes of assessing alkalinity and comparing it between strata and sites, the unit of measure reported by the laboratory, i.e., mg/L, was used.

Early season alkalinity was generally constant between sites and depth, with most measurements between 36 and 38mg/L. The one sample that reached 40mg/L was at the NB site on May 25<sup>th</sup> in the hypolimnetic sample.

The greatest variability between sites and depths came between June 23<sup>rd</sup> and August 16<sup>th</sup> (Fig. 17). Epilimnetic levels were between 44 and 46mg/L at all sites with the exception of the 64mg/L on August 16<sup>th</sup> at the NB site. Metalimnetic levels during this time were similar to epilimnetic levels.

Hypolimnetic alkalinity between June 23<sup>rd</sup> and August 16<sup>th</sup> was the most dynamic of the three strata over the season (Fig. 16). Over that time, levels at the NB site increased 50 to 54mg/L, and at the CL site, increased from 54 to 66mg/L. September 13<sup>th</sup> and October 12<sup>th</sup> levels were consistent across strata and sites, with hypolimnetic measurements between 40 and 42mg/L.

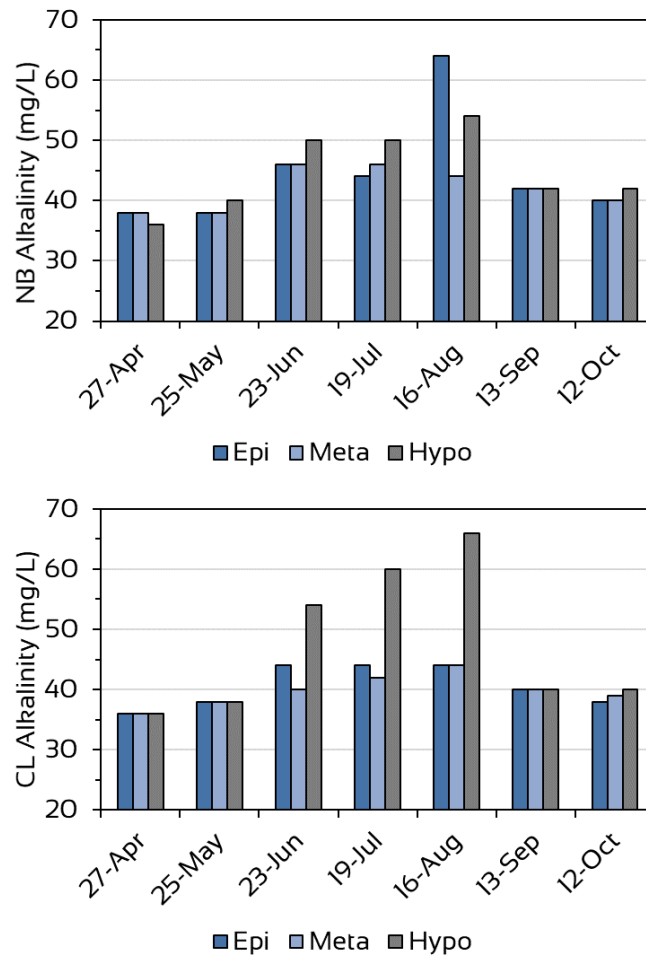


Figure 17. Alkalinity concentrations in the epilimnion (Epi), metalimnion (Meta), and hypolimnion (Hypo) at the North Bay Site (top), and Center Lake Site (bottom) of Bantam Lake in 2021.

The normal pH of surface waters of lakes in the Northeast can range from approximately 6 to 9 SU (standard units). Very low or very high pH levels will not support diverse fauna and flora in freshwater ecosystems. Algal community composition is influenced by pH. For example, the pH of the water will influence algae community characteristics by determining the type of dissolved carbon in the water column. At pH levels greater than 8.3, bicarbonate is the dominant form of carbon available to the pelagic algal community; the blue-green algae have adaptive advantages over other algal groups in those conditions in that they can efficiently utilize that form of carbon. Other algal groups are dependent upon carbon dioxide, which is more readily available in water below a pH of 8.3.

Epilimnetic pH in lakes is often higher than hypolimnetic pH, particularly as productivity increases. Carbon dioxide diffuses into the water from the atmosphere and is also a metabolic product of cellular respiration. Photosynthesis by algae and plants in the water utilize carbon dioxide in the water that might otherwise form carbonic acid, which is a weak acid. In the hypolimnion, the photosynthesis is light-limited, therefore carbonic acid levels are higher.

The pH was measured 17 times throughout the water column of all four sites in 2021. All data are in digital format. Below we report on data collected at the NB and CL sites, specifically from one meter of depth (epilimnetic pH), at the thermocline (metalimnetic pH), and at 0.5 meter from the bottom of the water column (hypolimnetic pH).

The average epilimnetic pH at the NB site was 8.1 SU. The minimum for the season was 7.4 SU and measured on October 12<sup>th</sup>. Ten of the epilimnetic measurements were >8 SU, and four were >8.3, which occurred on April 27<sup>th</sup>, July 16<sup>th</sup>, August 16<sup>th</sup>, and October 28<sup>th</sup>. The metalimnetic average, minimum, and maximum at the NB sites were 7.7, 7.1, and 8.1 SU, respectively. A metalimnetic pH of 8 to 8.1 SU was measured on April 27<sup>th</sup>, July 16<sup>th</sup>, and October 28<sup>th</sup>. Metalimnetic measurements in August were the lowest and all between 7 and 7.5 SU.

At the NB site, hypolimnetic pH was highest between April 27<sup>th</sup> and May 12<sup>th</sup>, and measured between 7.7 and 8.0 SU. Levels decreased to 7.0 SU by June 28<sup>th</sup>, and mostly oscillated between 7.0 and 7.3 SU through September 13<sup>th</sup>. On one occasion during that period, the season minimum of 6.7 SU was recorded on August 19<sup>th</sup> (Fig. 18). Between September 29<sup>th</sup> and October 28<sup>th</sup>, pH fluctuated between 7.2 and 7.6 SU.

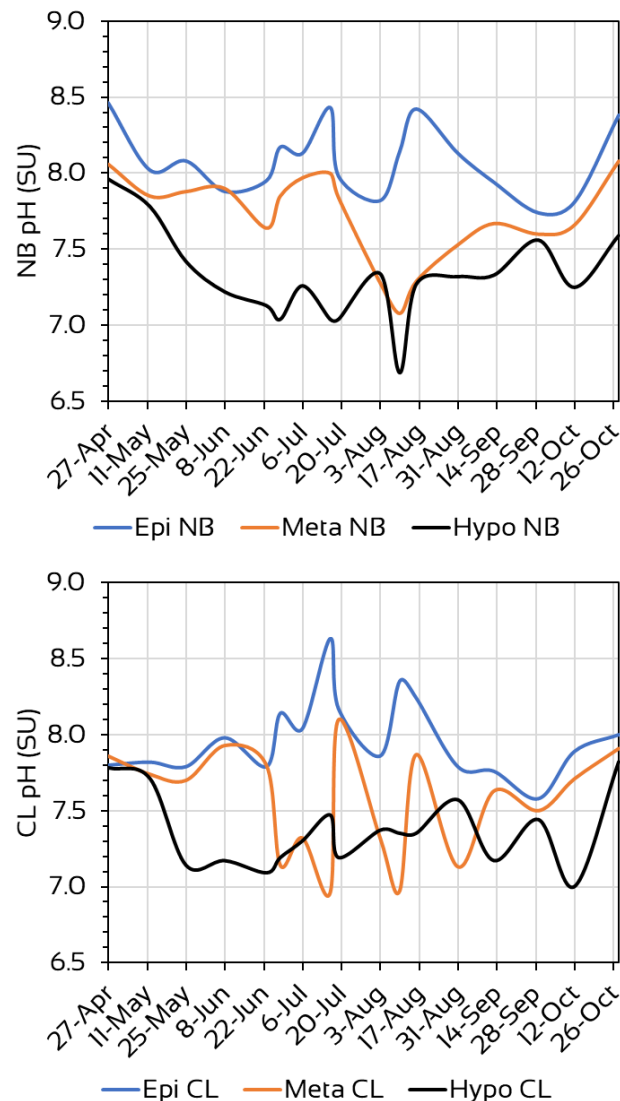


Figure 18. Epilimnetic (Epi), metalimnetic (Meta), and hypolimnetic (Hypo) pH at the North Bay (NB) site and CL site.

The average, minimum, and maximum pH in the epilimnion of the CL site were 8.0, 7.6, and 8.6 SU, respectively. Only the July 16<sup>th</sup> and August 10<sup>th</sup> did measurements exceed 8.3 SU. Six of the seven times an epilimnetic pH of >8.0 SU was measured were between June 28<sup>th</sup> and August 16<sup>th</sup> (Fig. 18). The minimum, maximum, and average metalimnetic pH values were 6.9, 8.0, and 7.6 SU, respectively. The period of greatest variability was between June 23<sup>rd</sup> and September 13<sup>th</sup>.

The CL hypolimnetic pH minimum, maximum, and average were 7.0, 7.8, and 7.4 SU, respectively. Levels in the beginning and end of the season were highest at 7.7 to 7.8 SU (Fig. 18). With one exception, all hypolimnetic pH measures were between 7.0 and 7.5 SU. The exception occurred on August 31<sup>st</sup> when a pH of 7.6 SU was measured.

### *Iron and Manganese*

Soluble iron and manganese concentrations in lake waters provide useful insights into the dynamics of the internal loading of phosphorus from anoxic lake sediments. In New England, oxidized iron compounds sequester phosphorus in lake sediments making it unavailable to the algae community in a particulated form. After depletion of oxygen in the surface sediments via aerobic cellular respiration, and provided that oxygen concentrations are not replenished, the microbial metabolic processes and composition of the microbes carrying out those processes shift.

Once oxygen is no longer available, other oxidizing agents are used sequentially in anaerobic respiration including nitrate, manganese, and iron. Once the iron compounds binding the phosphates are used, the iron and orthophosphates become soluble, diffuse, and accumulate in waters

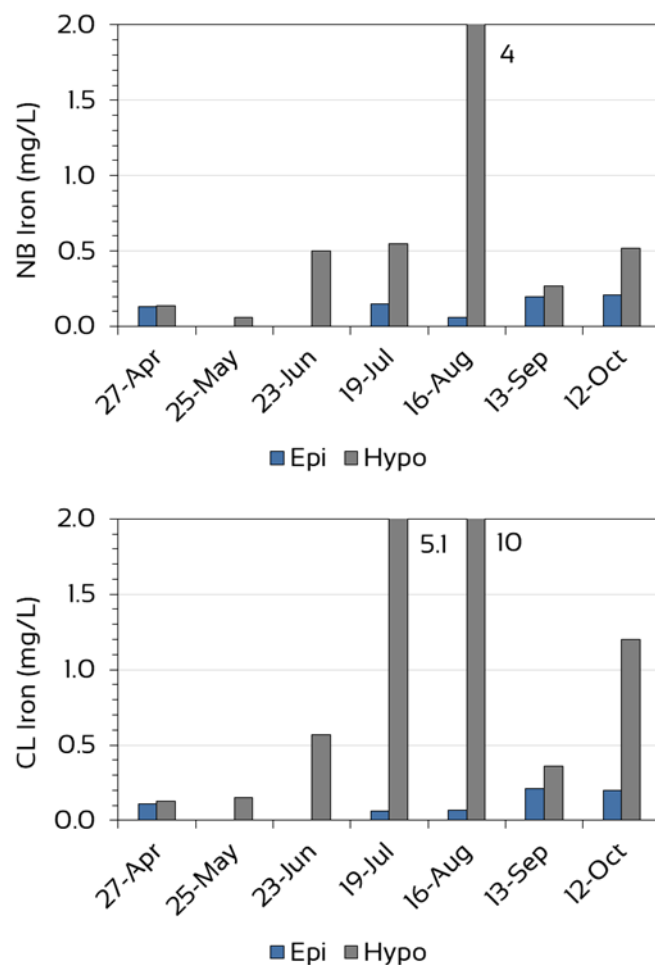


Figure 19. Epilimnetic (Epi) and hypolimnetic (Hypo) iron concentrations at the North Bay (NB; top) and Center Lake (CL; bottom) sites of Bantam Lake in 2021.

overlying the sediments. Although oxidized manganese compounds do not sequester phosphorus, they are the compounds used just before iron in the sequence of anaerobic oxidizing agent.

Early season epilimnetic ferrous iron ( $\text{Fe}^{2+}$ ) concentrations were undetectable to very low ( $\leq 0.13\text{mg/L}$ ) at both the NB and CL sites. Epilimnetic concentrations at the end of the season were higher, but still relatively low (0.2 to  $0.21\text{mg/L}$ ). The epilimnetic season average was 0.15 and  $0.13\text{mg/L}$  at the NB and CL sites, respectively

Early season hypolimnetic iron concentrations were also low (0.06 to  $0.15\text{mg/L}$ ). But concentrations increased exponentially to  $4.0\text{mg/L}$  by August 16<sup>th</sup> at the NB site, and to  $10.0\text{mg/L}$  by the same date at the CL site (Fig. 19). By the following sampling event – September 13<sup>th</sup> – concentration decreased to nearly early season levels. Hypolimnetic levels did increase again by October 12<sup>th</sup>, but only to  $0.52\text{mg/L}$  at the NB site, and to  $1.2\text{mg/L}$  at the CL site.

Epilimnetic manganese concentrations were relatively low and averaged  $0.03\text{mg/L}$  for the season at both sites. Early season concentrations of approximately 0.01 to  $0.02\text{mg/L}$  at both sites on April 27<sup>th</sup> and May 25<sup>th</sup> reached maximum concentrations of  $0.05\text{mg/L}$  on September 13<sup>th</sup> and October 12<sup>th</sup> at the NB site; maximums at the CL site occurred on the same dates but were 0.06 and  $0.07\text{mg/L}$ , respectively (Fig. 20).

Hypolimnetic manganese levels were similarly low on April 27<sup>th</sup> and May 25<sup>th</sup> at the NB site, but had increased by an order of magnitude to  $0.31\text{mg/L}$  by May 25<sup>th</sup> at the CL site. From June 23<sup>rd</sup> to August 16<sup>th</sup>, concentrations were highly elevated, reaching the season maximums of 1.6 and  $2.4\text{mg/L}$  by August 16<sup>th</sup>. Concentrations during that

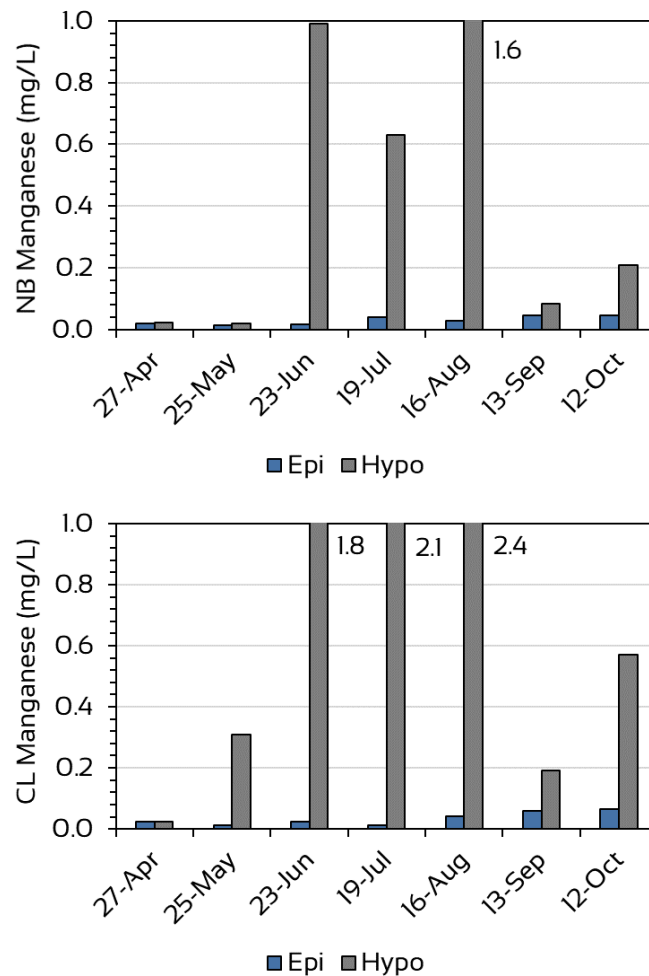


Figure 20. Epilimnetic (Epi) and hypolimnetic (Hypo) manganese concentrations at the North Bay (NB; top) and Center Lake (CL; bottom) sites of Bantam Lake in 2021.

three-month period were higher at the CL site (Fig. 20). By September 13<sup>th</sup> concentrations decreased to 0.09 and 0.19mg/L at the NB and CL sites, respectively, then modestly increased to 0.21 and 0.57mg/L at the respective sites.

## MAJOR FINDINGS

### *Phosphorus Mass Dynamics*

Since 2018, the lake average mass of total phosphorus in each stratum of the water column and for each date samples were collected was estimated (Fig. 21). Estimates were based on the consistent sampling of the strata as described in the *Methods* section of this report.

Concentrations at a stratum were multiplied by the volume of that stratum based on the hypso-graphic curve for the lake. The sum of the masses in each stratum on a given date provides an estimate for the entire water column, e.g., the mass of phosphorus in the entire water column on August 16<sup>th</sup> of 2021 was 1,231 kg (Fig. 21).

The April and May phosphorus levels theoretically represent importations of phosphorus from the watershed (i.e., the protracted period of time of hypolimnetic anoxia required for the internal loading process to initiate had not yet occurred). The masses in April of 2020 and 2021 are between two

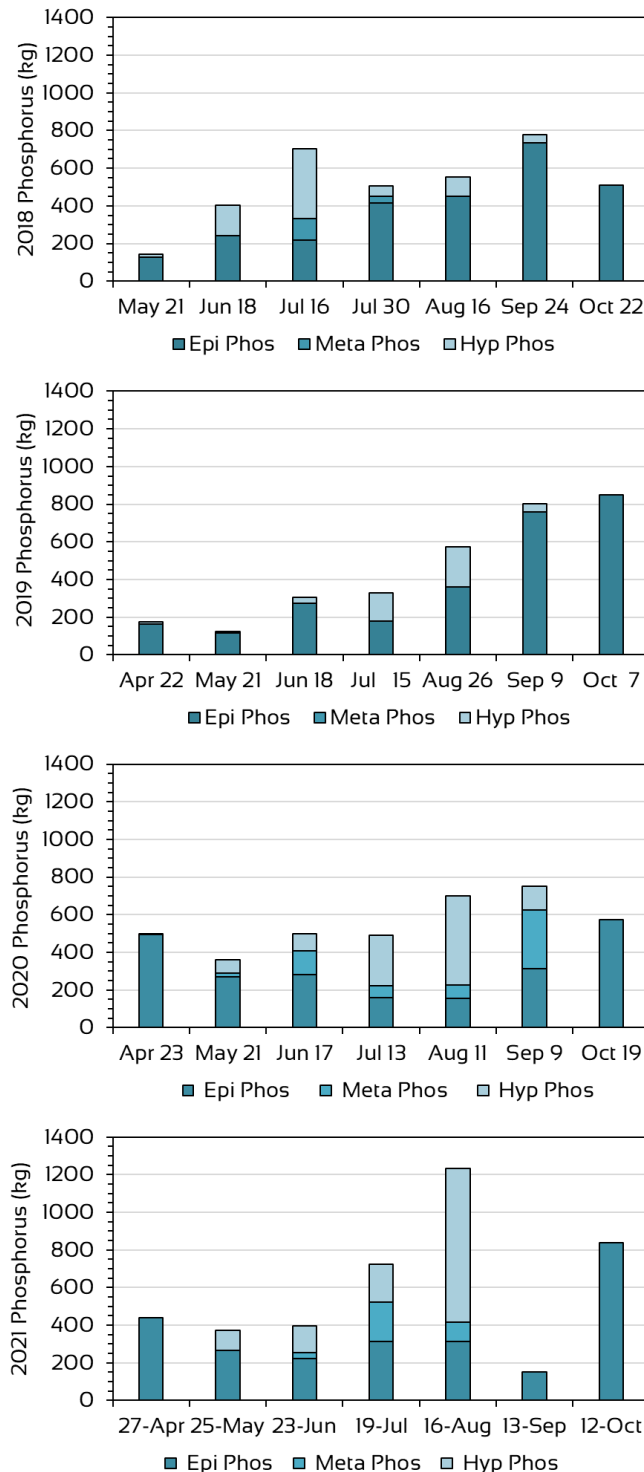


Figure 21. Mass of total phosphorus by strata (epi-limnion = Epi, metalimnion = Meta), and hypolimnion = Hypo) on each sampling event from 2018 to 2021.



and three times greater than the concentrations in 2018 (not depicted in Fig. 20) and 2019.

The recent two years have generally exhibited greater hypolimnetic phosphorus mass in mid-season months than in 2018 and 2019. The most conspicuous example is hypolimnetic phosphorus mass on August 16<sup>th</sup> of 2021 (Fig. 21). That date produced the single day maxima for the water column in the last four years.

The hypolimnetic phosphorus mass is a product of the phosphorus concentration and the volume of the strata and assumes the same concentration throughout the entire hypolimnetic strata. Each year since 2018 at the CL site, the August hypolimnion occupied the area from the 7m stratum to the bottom. The average hypolimnetic total phosphorus concentration in August has increased from 70.5µg/L in 2018, to 160 µg/L in 2019, to 255µg/L in 2020, to 282µg/L in 2021. We are unable to say with certainty why the hypolimnetic concentration has increased, but it may be related to the seasonal dynamics of stratification each year. Recent research using growing degree days to understand these dynamics shows promise (Kortmann and Cummins 2018) and may be useful in the future to provide a clearer picture on stratification at Bantam Lake.

Another noteworthy characteristic of the 2021 monthly total phosphorus mass balance was the conspicuous loss of phosphorus on September 13<sup>th</sup>; this loss was especially striking relative to water column phosphorus mass in September in the three preceding years (Fig. 21). One plausible explanation for the 2021 September phosphorus loss in the water column was the mixing and flushing of the lake by Tropical Storm Henri (August 22<sup>nd</sup>) and Hurricane Ida (September 2<sup>nd</sup>). Using a modified procedure to estimate watershed runoff (CWB 2020), we estimated that Hurricane Ida alone provided enough rain in the Bantam watershed to replace almost 40% of the lake's volume (WUWMCC 2021). The winds associated with both events would most certainly create an oxidized environment throughout much of the water column resulting in the precipitation of some of the phosphorus out of the water column.

Equally noteworthy was the recovery of the phosphorus in the water column by October 12<sup>th</sup>. The total mass for the water column was second only to that of August 16<sup>th</sup>, but may have been biased some by the phosphorus concentrations near the bottom of the water column (Fig. 7). The October 12<sup>th</sup> water column was not stratified and phosphorus concentrations at the 1m and middle stratum at both the NB and CL sites, and at the bottom of the NB water column were all between 25 and 28µg/L. The concentration at the bottom of the CL site on that date was 46µg/L despite oxygen concentrations of 9.2mg/L and ORP of 289mV.

### Compensation Depth and Cyanobacteria

As discussed earlier, the Compensation Depth is that depth where oxygen produced from algal photosynthesis is equaled to the oxygen consumed via algal cellular respiration. Kortmann (2015) discussed the position of the Compensation Depth relative to the metalimnion and thermocline as a variable in cyanobacteria positioning in the water column and as a stimulant of cyanobacteria growth. Water quality was likely to be good and unlikely to stimulate cyanobacteria productivity if the Compensation Depth extended below the thermocline. If the Compensation Depth was located within the metalimnion, a layer of cyanobacteria could form within that strata. Lastly, growth of cyanobacteria genera that can regulate buoyancy could be stimulated when the Compensation Depth is within the mixed epilimnetic layer. This implies the extension of anoxic waters into the bottom of the epilimnetic layer.

We examined this relationship at the NB, CL and PF sites in 2021 (Fig. 22). The Compensation Depths at the three sites was below the thermocline through late June. By early July, the Compensation Depth was above the thermocline at the CL and PF sites. That occurred at the NB site by mid-July.

The timing of high cyanobacteria cell counts and relative phycocyanin concentrations coincided with

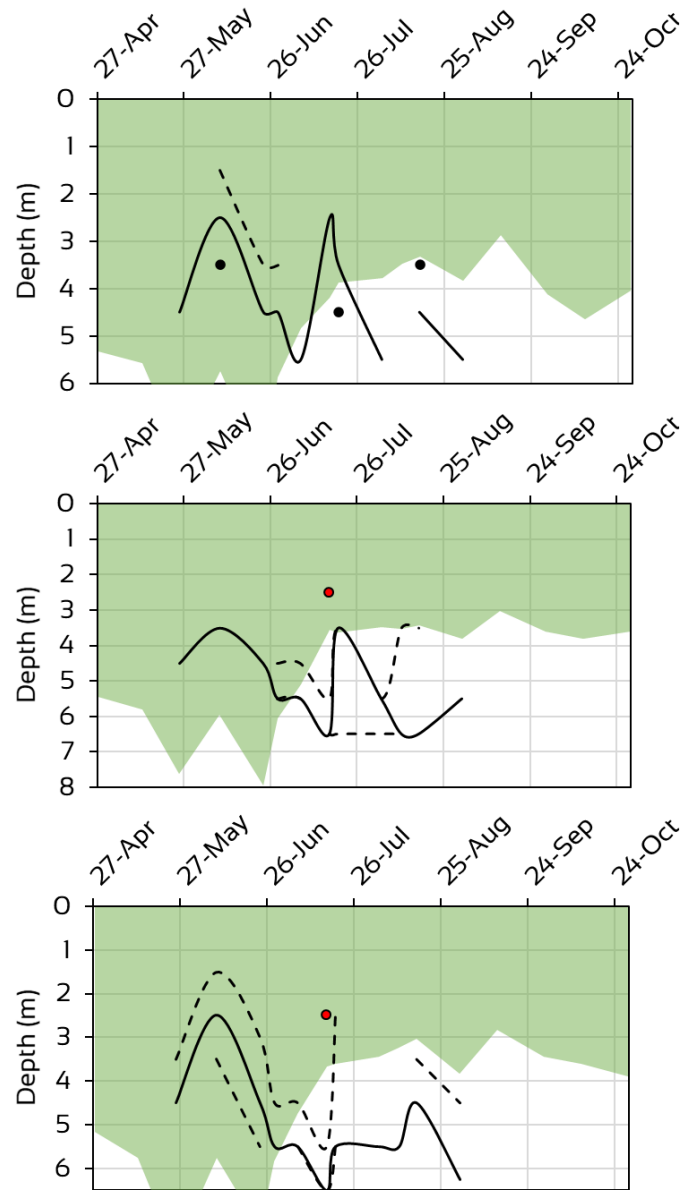


Figure 22. Area of the water column at the NB (top), CL (middle) and PF (bottom) sites above the Compensation Depth (shaded in green). The black dashed lines and black dots represent the upper and/or lower metalimnetic boundaries. The solid black line represents the location of the thermocline. The red dot on the CL and PF isopleths represents a second thermocline observed on at those two sites on July 16th.

the timing of observations of the Compensation Depth above the thermocline. Cyanobacteria genera that dominated Bantam Lake are capable of regulating buoyancy and include *Aphanizomenon spp.* and *Dolichospermum spp.* The data at Bantam Lake collected in 2021 does fit the model described by Kortmann (2015) for stimulation of cyanobacteria growth.

### *Water Column Stability and Cyanobacteria*

Last year we examined maximum RTRM scores in the water column to assess water column stability. Highly stable water columns with reduced mixing favors those cyanobacteria that can regulate buoyancy over other algae that rely upon less effective modes of remaining in the water column, e.g., high surface area to volume ratios. As a water column becomes more stable, the resistance to mixing at the thermocline tends to increase in strength. RTRM scores of <30 mean that layers are mixed; scores of  $\geq 30$  between strata are characteristic of the transitional metalimnion layer. RTRM scores of  $\geq 80$  between strata characterizes strong resistance to mixing (Siver et.al. 2018).

The maximum RTRM scores in the water column for the NB, CL, and PF sites were plotted to assess the stability of the water column during the 2020 and 2021 season (Fig. 23). As noted earlier, the 2020 season occurred during moderate to extreme draught conditions in Connecticut. There was one major storm event – Hurricane Isaias – that impacted Connecticut on August 4, 2020. In 2021, there were four major storm events: Tropical Storm Elsa on July 8<sup>th</sup>, Tropical Storm Fred on August 19<sup>th</sup>, Tropical Storm Henri on August 22<sup>nd</sup>, and Hurricane Ida on September 1<sup>st</sup>. The date of the 2020 and 2021 storm events were indicated on Figure 23.

It should be noted that there were four to eight more site visits in 2020 (25 visits to NB and CL; 20 to PF; and 21 to SB) than there were in 2021 (17 at each site). That aside, there did appear to be similarities in the maximum RTRM pattern from the start of each season through late June / early July. Afterwards, similarities diminished. In 2020, maximum RTRM values remain high through late July and decreased after Hurricane Isaias (Fig. 23). Even after Hurricane Isaias, RTRM at the CL site were not <80 until after August 19<sup>th</sup>.

Following Tropical Storm Elsa on July 8, 2021, there were substantial decreases in maximum RTRM values. Subsequently, maximum RTRM among the four sites was variable through late August. Following the three storms that occurred from August 19<sup>th</sup> to September 1<sup>st</sup>, maximum RTRM values decreased and the lake remained mixed for the remainder of the season.

It is well documented that the stratification and mixing processes – among other trophic variables – are important to the nutrient and algal dynamics in lakes. The 2020 and 2021 seasons provide good examples of how climate impacts the stratification and mixing process. However, despite differences in the patterns of maximum RTRM values (i.e., patterns of mixing and stratification) between the two years, both

years experienced impairments from cyanobacteria blooms and the BPAC implemented two copper sulfate treatments each season to manage cyanobacteria levels. While water column stability and mixing are important, it appears that those variables do not impact algal dynamics independently at Bantam Lake.

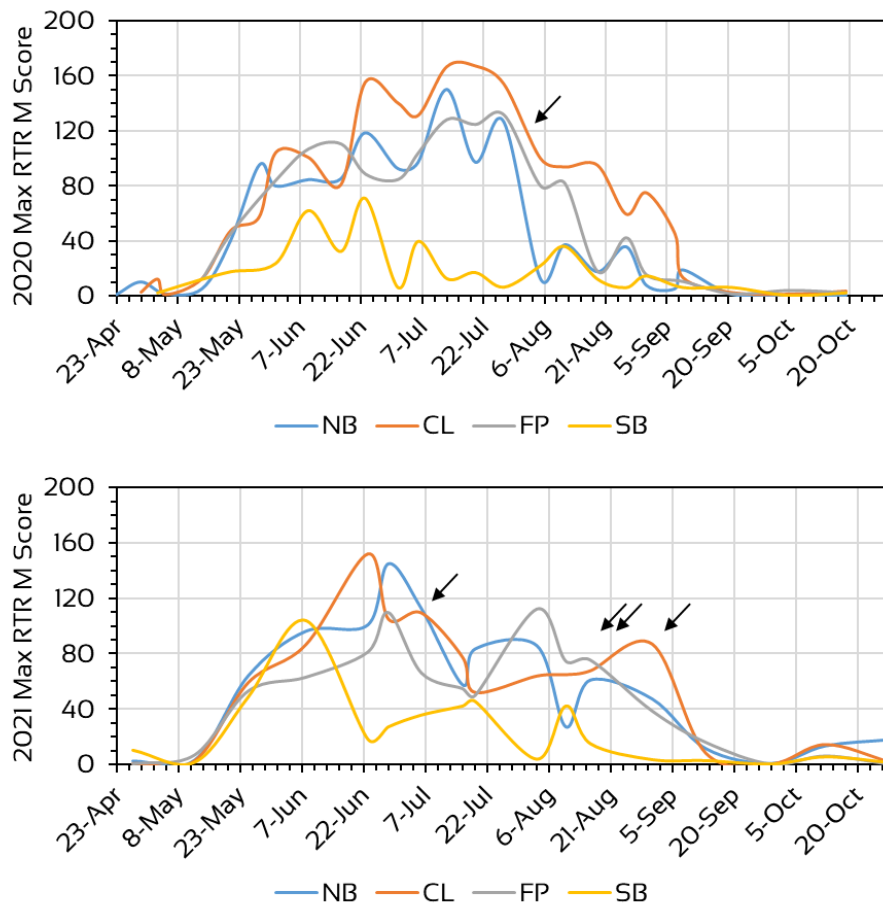


Figure 23. Maximum RTRM scores plotted over time in the water column of the North Bay (NB), Center Lake (CL), Folly Point (FP), and South Bay (SB) sites during the 2020 (top) and 2021 (bottom) seasons. Arrows indicate storm events: in 2020 the arrow denotes Hurricane Isaias; in 2021 from L to R, arrows denote Tropical Storm Elsa, Tropical Storm Fred, Tropical Storm Henri, and Hurricane Ida.

### Cyanobacteria Productivity

There is an ongoing, nationwide program to collect data on cyanobacteria populations across the country to better understand the increases in bloom frequency and intensity. CyanoMonitoring utilizes lake scientists and lake managers – as well as citizen scientists – to collect samples and analyze them with fluorimetry in a manner similar to that discussed in earlier sections of this report (CMC 2021).

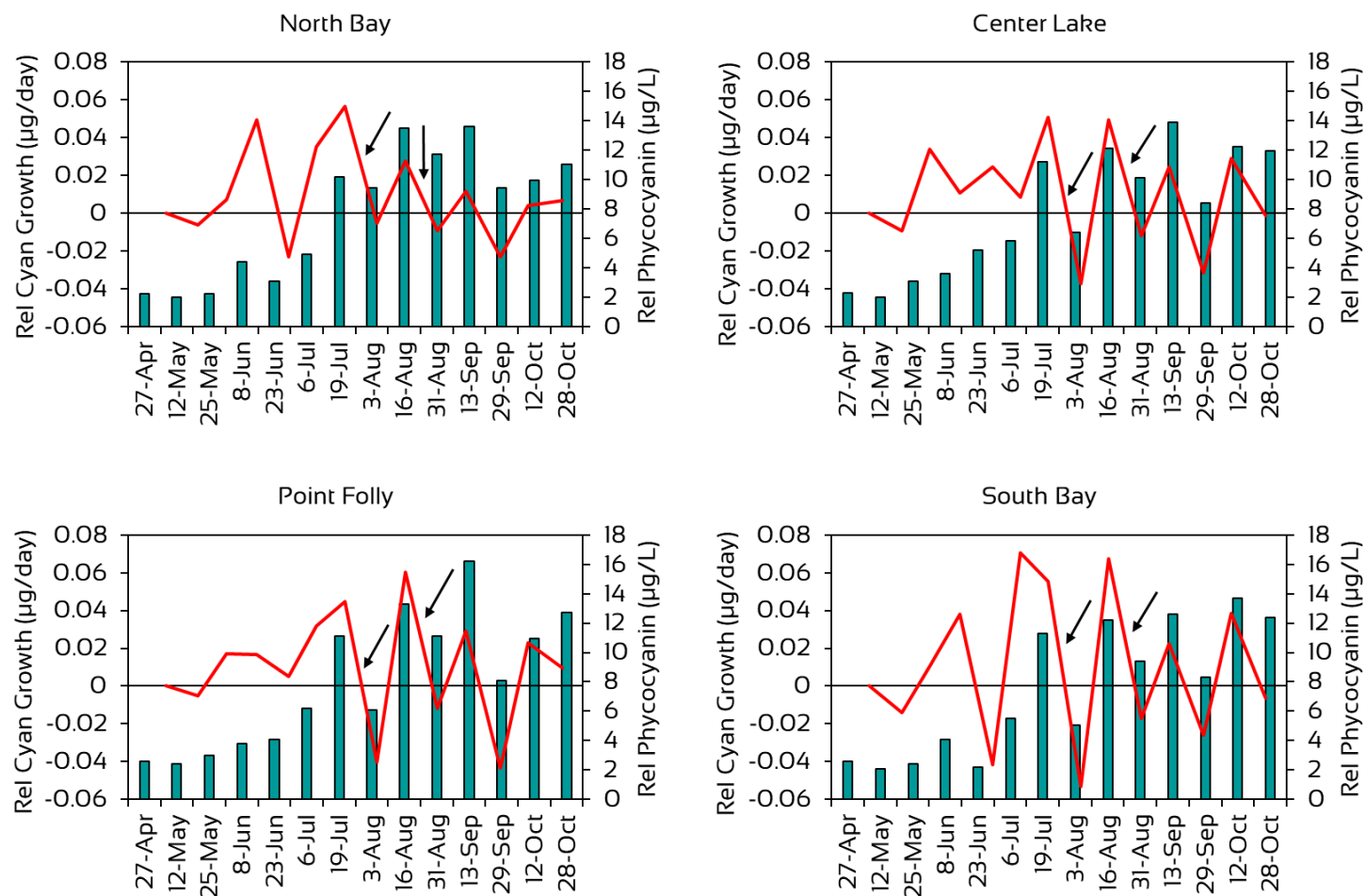


Figure 24. Relative cyanobacteria growth rates (Rel Cyan Growth; red line) and relative phycocyanin concentrations (Rel Phycocyanin; cyan bars) at the four sites on Bantam Lake during the 2021 sampling season. Black arrows point to growth rates following the 2021 copper sulfate treatments of July 29<sup>th</sup> and August 24<sup>th</sup>.

The USEPA provides to CyanoMonitoring practitioners the following formula to calculate cyanobacteria growth rates:

$$\mu \text{ d}^{-1} = \ln(F_2/F_1)/(t_2-t_1)$$

where  $\mu \text{ d}^{-1}$  is growth in micrograms per day;  $F_2$  is the fluorescence at time 2 ( $t_2$ ); and  $F_1$  is the fluorescence at time 1 ( $t_1$ ). We were also advised to assess growth rates in light of actual pigment measurements (Nancy Leland, UNH, personal communication, December 13, 2021). Whereas CyanoMonitoring fluorimetrically analyzes phycocyanin in different cyanobacteria size fractions (e.g., large bloom-former genera vs small picoplankton genera), we utilized relative phycocyanin measured in-situ at the four sites, and plotted concentrations and growth rates together (Fig. 24). In addition, we have noted on the timeline when copper sulfate treatments occurred.

Seasonal growth rate patterns were similar at the CL and PF sites. Growth rates generally increases through July 19<sup>th</sup> when relative phycocyanin concentrations exceeded 10 $\mu\text{g/L}$  and before the first copper sulfate treatment. Growth substantially decreased following the July 29<sup>th</sup> treatment but rebounded quickly before the next treatment on August 24<sup>th</sup>; following, the concentration decreased for the remainder of the season. Although the highest relative phycocyanin concentrations occurred on September 13<sup>th</sup>, the increase in growth following the second treatment was not as substantial as was the growth following the first treatment (Fig. 24).

The NB site exhibited a similar pattern with the following exceptions. First, there was a striking growth rate decrease early in the season following June 8<sup>th</sup> that was not observed at the CL and PF sites. That decrease was followed by a substantial increase after June 23<sup>rd</sup>. The other exception was the more modest growth rate reduction following treatments.

The growth rate pattern at the SB site was similar to those at the CL and PF sites after August 16<sup>th</sup>. The pattern prior to August 16<sup>th</sup> differed from the other sites in terms of the magnitude of the changes in growth (Fig. 24). The decrease in growth following the July 29<sup>th</sup> treatment was the single greatest decrease between two consecutive sampling dates at any site through out the season.

### *Other Considerations of Cyanobacteria Genera*

Earlier we described inconsistencies between cyanobacteria cell concentrations and relative phycocyanin at end of season (see *Cyanobacteria Cell Concentrations and Relative Biomass*). We hypothesize that some of the discrepancy may be due to the seasonal change in dominant cyanobacteria genera. For much of the season, the filamentous *Aphanizomenon spp.* was the dominant genus. While cells at the end of the filaments tend to be elongated, most of the cells are small in size and volume.

At the end of the season, *Aphanizomenon spp.* decreased in importance while other genera, e.g., *Dolichospermum spp.*, became more important. Also filamentous, *Dolichospermum spp.* cells are large in comparison to *Aphanizomenon spp.* with greater biovolume. This could account for some of the decrease in cell concentrations without a proportional decrease in relative phycocyanin concentration. Additionally, we do not account for the quantity of most picoplankton size (<2µm in diameter) cyanobacteria given the difficulty to identify them, but their phycocyanin is measured as part of the whole water relative concentration. An increase in the number of picoplankton sized cyanobacteria near the end of the season could also contribute the decreased in cells counted but not in relative phycocyanin levels.

We reported that, despite high cyanobacteria cell concentrations, Microcystin levels were always low. We also reported that Microcystin is one of nine types of cyanotoxins and the one that is recommended for monitoring because it is the most common in freshwater systems; and, that the Microcystin-LN congener is considered one of the most toxic of all the cyanotoxins. However, *Aphanizomenon spp.* has not been associated with Microcystin. Instead, this genus is associated with Anatoxin, Saxitoxin, and Cylindrospermopsin (Cheung et. al. 2013, CT DPH & CT DEEP 2019). Testing for the other toxins during the height of *Aphanizomenon spp.* productivity in the future could be useful in assessing all risks from cyanotoxins.

Last year we hypothesized that allochthonous phosphorus associated with spring watershed runoff may have resulted in the 2020 spring *Aphanizomenon* bloom. In April of 2021, total phosphorus concentrations were on average >25µg/L (Fig. 7), the relative abundance of *Aphanizomenon spp.* by May 25<sup>th</sup> was 41% at NB and 27% at CL, but cell concentrations were low (<5,000 cells/mL).

An alternative hypothesis to explain the early season *Aphanizomenon* bloom in 2020 was that this genus overwintered in the water column due to a mild winter (R. Kortmann, personal communication, December 16, 2021). A similar scenario was documented at nearby Lake Waramaug (Kortmann 2021).

Lastly, we reported average epilimnetic and metalimnetic total phosphorus concentrations that theoretically supported mesotrophic algal productivity, and not the eutrophic conditions regularly observed at Bantam Lake. However, the dominant cyanobacteria at Bantam Lake are those capable regulating buoyancy (e.g., *Aphanizomenon spp.*, *Dolichospermum spp.*, *Planktothrix spp.*); therefore, are potentially capable of harvesting phosphorus from hypolimnetic depths where the concentrations were characteristic of eutrophic conditions at the NB site, and of highly eutrophic conditions at the CL site.

Last year, we listed findings supporting internal loading of phosphorus as a likely significant contributor (if not the most significant contributor) to algal bloom conditions at Bantam Lake. These finding included:

- Elevated hypolimnetic total phosphorus concentrations;



- Anoxic conditions and ORP of <200mV at deeper depths;
- Elevated ammonia, manganese, and ferrous iron at the lower depths;
- Dissimilatory reduction of compounds such as nitrate and sulfate during anaerobic cellular respiration resulting in the generation of alkalinity, which was also elevated at the lower depths; and
- Elevated specific conductance at the lower depths.

These characteristics of the Bantam Lake water quality are still relevant in 2021. It is also worth noting that the dissimilatory reduction processes at the bottom can result in loss of phosphorus binding sites once bottom waters are oxygenated.

### *Other Water Quality Characteristics*

In Table 5, we have compiled averaged Bantam Lake water quality data collected by AER (2018 to 2021), as well as averages from the 1990s collected by Canavan and Siver (1994, 1995). Also provided are averages for lakes in the Western Uplands of Connecticut, which includes Bantam Lake, compiled in the same 1990s study.

Data compiled from the 1990s study were based on four summer visits to one site between 1991 and 1993, and not on the seven visits each year to two sites in the years from 2018 to 2021. This may explain some of the differences between recent conditions and those recorded in the 1990s.

A comparison of average conditions from 2018 to 2021 suggests that while the lake is eutrophic, it appear to be stable. Some variability is noted in some parameters, including total nitrogen and specific conductance. However, the differences do not appear to be significant and/or unidirectional. Stable conditions are obviously preferred to continued decline. The current stability may be due, in part, to the efforts of the BLPA, the CT DEEP, and others who promote and initiate efforts to protect water resources.

Last year we displayed hypolimnetic ferrous ( $\text{Fe}^{+2}$ ) iron concentrations to illustrate the timing of phosphorus loading. Below we have appended 2021 to those data (Fig. 25). As in past years, the 2021 CL levels reach a much higher maximum level by August than did the NB levels. Concentrations in 2021 appear to follow a pattern similar to that of 2018, but also reach a maximum concentrations similar to that observed in 2020.

Table 5. Average water quality characteristics in the epilimnion of Bantam Lake from the early 1990s, 2018, 2019, 2020, and 2021. Also provided are averages for lakes in the Connecticut Western Uplands based on a 1990s study (Canavan & Siver 1994, 1995). The 1990s data is also from that study.

Parameter	Units	Bantam Lake					Western Uplands Lakes		
		1990s	2018	2019	2020	2021	Min	Max	Mean
Total Nitrogen	µg/L	714	550	276	469	459	208	714	364
Total Phosphorus	µg/L	42	22.5	22.7	22.8	23.6	10	57	33
Chlorophyll- <i>a</i>	µg/L	19.7	9.2	9.8	8.5	8.0	0.7	19.7	5.1
Secchi Disk	meters	1.7	2.28	2.66	2.10	2.27	1.7	7.6	3.5
pH	SU	7.8	7.8	8.0	8.4	8.0	4.6	8.1	7.2
Sp. Conductivity	µS/cm	122	189	176	187	192	25	188	96
Alkalinity	mg/L	30.5	40.7	39.4	39.7	42.6	23.7	44	21
Chloride	mg/L	10.3	33.7	27.9	28.5	27.4	0.7	24.1	9.2
Calcium	mg/L	8.2	11.9	10.5	11.6	11.7	2.8	11.4	6.8
Magnesium	mg/L	7.8	4.8	4.2	5.1	4.9	1	5.2	4.1
Sodium	mg/L	7.4	17.2	15.5	15.8	14.7	1.4	10.4	5.3
Potassium	mg/L	1.2	1.9	1.5	1.2	ND	0.2	0.9	0.5

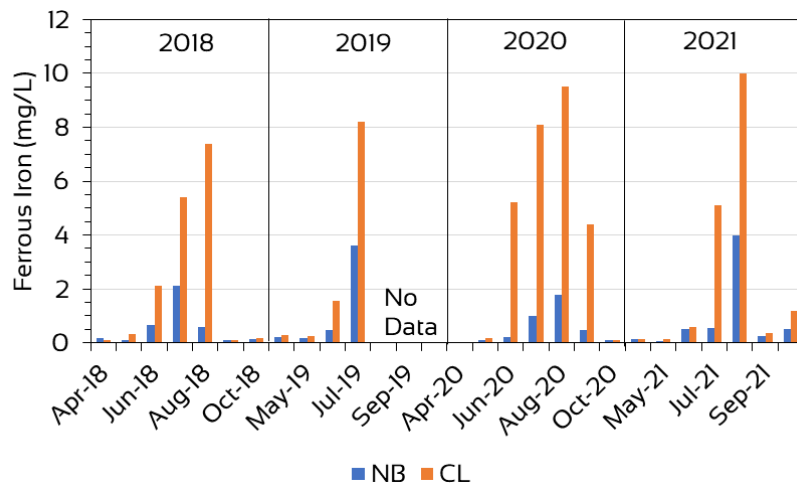


Figure 25. Ferrous iron concentrations in the hypolimnion of the North Bay and Center Lake sites in the 2018, 2019, 2020, and 2021 seasons. Data not available for August 26 – October 7, 2019.

## RECOMMENDATIONS

1. Bantam Lake is a locally and regionally important inland water resource where cyanobacteria blooms and aquatic invasive plant populations are actively managed. Active management necessitates water quality monitoring to document positive outcomes and detect negative consequences should they occur. Additionally, the State's TMDL study and watershed-based plan advises continued water quality monitoring of Bantam Lake. We support that recommendation with the following changes:
  - a. Eliminate iron and manganese analyses. These have provided useful information in the past but will not likely provide any additional insights in the future.
  - b. Reduce base cation and anion sampling and analyses to three times a year (April, June, and August). These parameters tend to be conservative and change slowly over time.
2. The BLPA has amassed a substantial water quality database over the years worthy of a rigorous statistical analysis to detect trends. These data could be compiled and analyzed with methods such as multiple linear regression and Analyses of Variance to understand if and how the lake has changed within the timeframe of those data collections.
3. As noted earlier, Microcystin levels measured at Bantam Lake are within levels considered safe. However the dominant cyanobacteria genus, *Aphanizomenon spp.*, is not known to synthesize that toxin. During the peak of *Aphanizomenon* growth in the future, samples could be analyzed for Anatoxin and Saxitoxin, which *Aphanizomenon spp.* are known to produce.
4. The State's TMDL study prescribes a rigorous lake and watershed monitoring program. A quality assurance project plan is an excellent means of assuring continuity in data collections over time and should be developed for Bantam Lake and its watershed.

## REFERENCES

- [BLPA] Bantam Lake Protective Association. 2021. Bantam Lake Cyanos. <https://bantam-lakecyanos.blogspot.com/>
- Bell, M. 1985. The Face of Connecticut. State Geological and Natural History Survey of Connecticut. Bull. 110.
- Burford M.A, Carey C.C, Hamilton D.P., Huisman J., Paerl H.W, Wood S.A, Wulff A. 2020. Perspective: Advancing the research agenda for improving understanding of cyanobacteria in a future of global change. Harmful Algae. 91. <https://www.sciencedirect.com/science/article/abs/pii/S1568988319300514?via%3Dihub>
- [CWB] California Water Boards. 2022. Guidance Compendium for Watershed Monitoring and Assessment. [https://www.waterboards.ca.gov/water\\_issues/programs/swamp/docs/cwt/guidance/512.pdf](https://www.waterboards.ca.gov/water_issues/programs/swamp/docs/cwt/guidance/512.pdf)
- Canavan RW, Siver PA. 1994. Chemical and physical properties of Connecticut lakes, with emphasis on regional geology. LAKE RESERV MANAGE. 10(2):175-188.
- Canavan RW, Siver PA. 1995. Connecticut Lakes: A study of the chemical and physical properties of fifty-six Connecticut Lakes. New London (CT): Connecticut College Arboretum.
- Cheung MY, S Liang, and J Lee. 2013. Toxin-producing Cyanobacteria in Freshwater: A Review of the Problems, Impact on Drinking Water Safety, and Efforts for Protecting Public Health. Journal of Microbiology (2013) Vol. 51, No. 1, pp. 1–10. <http://www.ilakes.org/ch/web/s12275-013-2549-3.pdf>
- [CT DEP] Connecticut Department of Environmental Protection. 1991. Trophic Classifications of Forty-nine Connecticut Lakes. CT DEEP, Hartford, CT. 98 pp.
- [CT DPH and CT DEEP] Connecticut Department of Public Health and Connecticut Department of Energy and Environmental Protection. 2019. Guidance to Local Health Departments for Blue–Green Algae Blooms in Recreational Freshwaters. [https://portal.ct.gov/-/media/Departments-and-Agencies/DPH/dph/environmental\\_health/BEACH/Blue-Green-AlgaeBlooms\\_June2019\\_FINAL.pdf?la=en](https://portal.ct.gov/-/media/Departments-and-Agencies/DPH/dph/environmental_health/BEACH/Blue-Green-AlgaeBlooms_June2019_FINAL.pdf?la=en)
- [CT DEEP] Connecticut Department of Energy and Environmental Protection. 2020. Integrated Water Quality Report to Congress. <https://portal.ct.gov/DEEP/Water/Water-Quality/Water-Quality-305b-Report-to-Congress>
- [CT DEEP] Connecticut Department of Energy and Environmental Protection. 2021. The Connecticut Total Maximum Daily Load (TMDL) Program. <https://portal.ct.gov/DEEP/Water/TMDL/Total-Maximum-Daily-Load>
- [CMC] Cyanobacteria Monitoring Collaborative. 2021. <https://cyanos.org/>
- Deevey ES Jr. 1940. Limnological studies in Connecticut. V. A contribution to regional limnology. AM J SCI. 238(10):717-741.
- Frink CR. 1991. Estimating nutrient exports to estuaries. J. Environ. Qual. 20:717-724.
- Frink CR, Norvell WA. 1984. Chemical and physical properties of Connecticut lakes. New Haven (CT): Connecticut Agricultural Experiment Station. Bulletin 817. 180 pp



Healy DF and KP Kulp. 1995. Water Quality Characteristics of Selected Public Recreational Lakes and Pond in Connecticut. US Geological Survey Water-Resource Investigations Report 95-4098. 227pp.

Ho JC, Michalak AM, & Pahlevan N. 2019. Widespread global increase in intense lake phytoplankton blooms since the 1980s. *Nature*. 574: 667–670.

<https://doi.org/10.1038/s41586-019-1648-7>

Jacobs RP, O'Donnell EB. 2002. A fisheries guide to lakes and ponds of Connecticut, including the Connecticut River and its coves. Hartford (CT): Connecticut Department of Energy and Environmental Protection, Bulletin No. 35.

Kortmann, RWP. 2015. Cyanobacteria in Reservoirs: Causes, Consequences, Controls. *J New England Water Works Assoc.* 129(1):73-90.

Kortmann, RWP. 2020. Managing Reservoir Stratification in a Variable Climate. *J New England Water Works Assoc.* 135(1):31-52.

Kortmann, RWP and Cummins, E. 2018. Climate Change in the Northeast: What Might It Mean to Water Quality Management? *J New England Water Works Assoc.* 132(4):236-254.

<https://www.nxtbook.com/naylor/NEWQ/NEWQ0418/index.php?startid=236#/p/236>

Lawton L., Marsalek B., Padisák J., Chorus I. 1999. DETERMINATION OF CYANOBACTERIA IN THE LABORATORY. In *Toxic Cyanobacteria in Water: A guide to their public health consequences, monitoring and management*. Chorus and Bartram, eds.

McMaster NL & DW Schindler. 2005. Planktonic and Epipelagic Algal Communities and their Relationship to Physical and Chemical Variables in Alpine Ponds in Banff National Park, Canada, Arctic, Antarctic, and Alpine Research, 37:3, 337-347, DOI: 10.1657/1523-0430(2005)037[0337:PAEACA]2.0.CO;2

[NIDIS] National Integrated Drought Information System. 2021. Drought in Connecticut from 2000–Present. <https://www.drought.gov/states/connecticut#historical-conditions>

Redfield A.C. 1958. The biological control of chemical factors in the environment. *American Scientist*. 46(3):205-221.

Siver PA .1992. Assessing historical conditions of Bantam Lake, Connecticut, using a paleolimnological technique. Report to the Town of Morris, Connecticut

Siver, P.A. 1993. Inferring lakewater specific conductivity with scaled chrysophytes. *Limnol. Oceanogr.* 38: 1480-1492

Siver PA & Marsicano LJ. 1996. Inferring lake trophic status using scaled chrysophytes. In: *Chrysophytes: Progress and New Horizons*. Kristiansen J, Cronberg G (eds) Beihefte zur Nova Hedwigia 114: 233-246

Siver, P.A., Canavan, R.W. IV, Field, C., Marsicano, L.J. and A.M. Lott. 1996. Historical changes in Connecticut lakes over a 55-year period. *Journal of Environmental Quality* 25: 334-345.

Siver PA., Lott AM, Cash E, Moss J and Marsicano LJ. 1999. Century Changes in Connecticut, U.S.A., Lakes as Inferred from Siliceous Algal Remains and

Their Relationships to Land-Use Change. *Limnol. and Oceanogr.* 44(8):1928-1935

Siver P., Marsicano L., Lott A., Wagener S., Morris N. 2018. Wind induced impacts on hypolimnetic temperature and thermal structure of Candlewood Lake (Connecticut, U.S.A.) from 1985–2015. *Geo: Geography and the Environment*. 5(2). <https://doi.org/10.1002/geo2.56>

Søndergaard, M., 2009. Redox Potential. In *Encyclopedia of Inland Waters* ed. Gene Likens. Academic Press.

[US EPA] United States Environmental Protection Agency. 2014. Cyanobacteria and Cyanotoxins: Information for Drinking Water Systems. [https://www.epa.gov/sites/default/files/2014-08/documents/cyanobacteria\\_factsheet.pdf](https://www.epa.gov/sites/default/files/2014-08/documents/cyanobacteria_factsheet.pdf)

[US EPA] United States Environmental Protection Agency. 2020. Health Effects from Cyanotoxins. <https://www.epa.gov/cyanohabs/health-effects-cyanotoxins>

[USEPA] United States Environmental Protection Agency. 2021. Health Effects from Cyanotoxins. <https://www.epa.gov/cyanohabs/health-effects-cyanotoxins>

Weather Underground – White Memorial Conservation Center. 2021. <https://www.wunderground.com/dashboard/pws/KCTLITCH9>

Wetzel RG. 2001. *Limnology Lake and River Ecology*. 3<sup>rd</sup> Ed. Academic Press. 1006 pp.